Aalborg Universitet

Wavestar Energy Production Outlook

Frigaard, Peter Bak; Andersen, Thomas Lykke; Kofoed, Jens Peter; Kramer, Morten Mejlhede; Ambühl, Simon

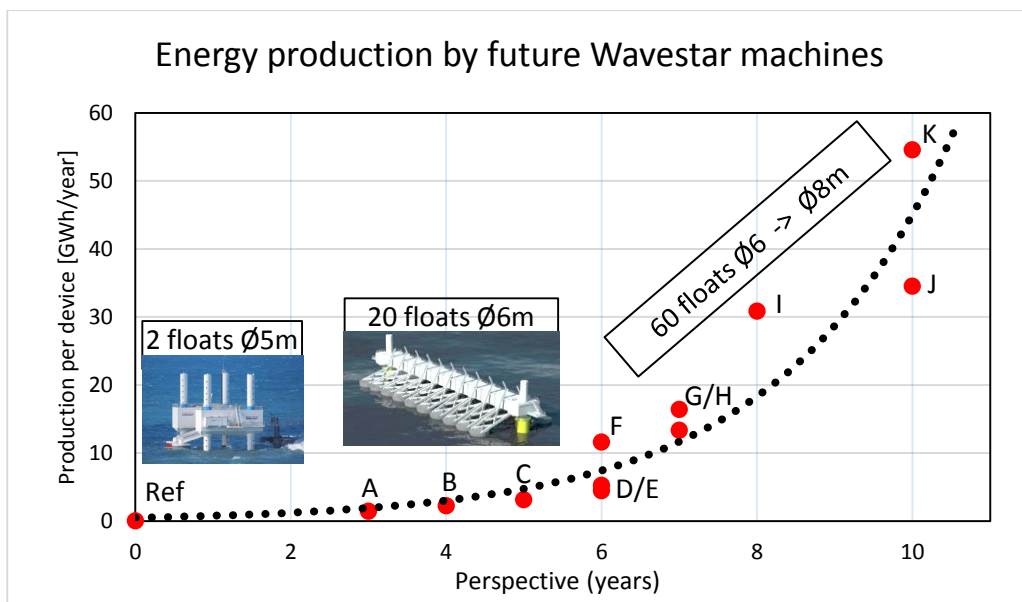# Wavestar Energy Production Outlook

Peter Frigaard

Thomas Lykke Andersen

Jens Peter Kofoed

Morten Kramer

Simon Ambühl

Aalborg University

Department of Civil Engineering

Wave Energy Research Group

DCE Technical Report No. 201

February 2016

Contents

1 Introduction

It is of paramount importance to decrease the Cost of Energy (CoE) from Wavestar wave energy converters (WECs) in order to make the WECs competitive to other sources of renewable energy. The CoE can be decreased by reducing the cost of the machines (CAPEX and OPEX) and by increasing the income. The income can most obviously be enlarged by increasing the energy production. The focus of the present note is solely on expectations to the yearly energy production from future Wavestar WECs.

Aalborg University (AAU)[1] has for 15 years extensively studied the Wavestar WECs both by using numerical models and experimental assessments within a wide range of engineering disciplines. Only work related to the energy production of Wavestar WECs will be referred here, and a look-back on this work is given in Section 3. The current configuration of the Wavestar WEC termed "Wavestar C6" is a machine with 20 floats each having a diameter of 6 meters. Significant efforts have been spend on modelling and validating the production from this device, so there is a strong confidence in the production estimates particularly for this configuration. Over the years of investigation the energy production of the Wavestar WECs has increased by more than a factor 3 to the current level, but as described in Section 4 there are still many possibilities for further significant improvements and optimisations of the power production. In Section 5 future cases are defined where such improvements are quantified by adjusting coefficients in the prediction model used for the production estimates. Only very small adjustments are done not to "promise too much" and to give confidence in that the benefit can be achieved with only few years of further development (say 3-10 years). As the geographical locations of the WECs are of high importance for the production, the chosen sites are described in detail in Section 6 and 7. In Section 8 the model used for the production estimations are given, and by using the power matrices presented in Section 9 the expected yearly production for the cases are presented in Section 10. Some brief conclusions are presented in the following section.

A parallel can be drawn to the wind energy development. In 1980 the first wind turbines was about 10 kW, but since then an exponential increase in the power production has taken place over the years, and today the biggest wind turbine produces almost 1000 times more (Vestas V164 from 2014 is 8 MW). Such increase was not foreseen by even the most optimistic researchers in the childhood for the wind energy, and the example illustrates that the future for such development is difficult to predict.

Future Wavestar machines are expected to follow a somewhat similar tendency as for wind power. In 2009 Wavestar installed the 110 kW Hanstholm prototype. Future machines will be larger and increases in the production will for sure take place, and Wavestar WECs in the higher MW-range can with time be developed. This note provides production estimates for such future machines for a development within a time frame of about 10 years by describing machines up to 15 MW capacity, although the progress may continue beyond this by building devices with even higher capacity.

The cost of the machines (CAPEX and OPEX) for the different cases at the chosen locations will be very different. The costs must be calculated and used in a Cost of Energy calculation to determine which of the cases and sites that are most suitable for installing Wavestar WECs. It is out of the scope of the present report to perform this investigation.

---

[1] The Wave Energy Research Group at Aalborg University (AAU) performs R&D within the wave energy field and has established itself as a R&D hub connecting all Danish, as well as a number of international, concepts. Since the group started its activities about 20 years ago, AAU has worked with wave theory, resource assessment and numerical modelling; with the hydrodynamics, power conversion systems and mechanical parts of WECs; and with the testing and evaluating of 25 WECs at AAU wave tank facilities and in real sea [16, 48].
http://www.waveenergy.civil.aau.dk/

2 Conclusions

Model predictions for 11 cases (*Case A..Case K*) with increasing production is presented in the report by investigating larger machines with additional floats at more exposed sites. In addition justified improvements in the design, control and power take off efficiency are quantified and incorporated in the prediction model in order to take into account benefits which are expected through future R&D.

It is shown that a 20-float **Demonstrator** machine with 6 m floats located by the site Mermaid in Belgium may initially produce 1.4 GWh/year (*Case A*), but that this level by some years with further optimization and improvements could be increased up to 3.1 GWh/year (*Case C*). If the development is continued and a similar configured **pre-commercial or commercial** device is placed in a French wave environment the production could be up to 5.3 GWh/year (*Case E*). To extend the production further the number of floats is first increased to 60, and a production of up to 16.4 GWh/year is predicted (*Case H*) for a **commercial** device at a French exposed site. In the last cases the production is further increased by making larger machines with larger floats, such that the machine is equipped with 60 floats each having a diameter of 8 m. In these cases the machine may produce about 35 GWh/year (*Case J*) for a fixed bottom standing one located in UK, but if the device is placed at a very exposed condition at 100 m water depth such a machine may produce up to 55 GWh/year (*Case K*). A floating WEC is presumably needed in order to survive at such a high water depth.

> The outlook reaches from 3 to 10 years into the future, revealing a potential yearly production per Wavestar device stating at 1.4 GWh and reaching 55 GWh.
> The authors recommend that the forthcoming R&D is focussing on realization of *Case H*, where a yearly production of **16.4 GWh** can be achieved in about 7 years.

The presented cases reach only about 10 years into the future (*Case K*), but the development may continue beyond this by building larger and more optimal machines allowing further increases in the energy production. The wave resource at higher depth at more exposed sites than the ones included in this report may most likely justify building machines with float diameters of 10 to 12 m, or even larger. The future offshore wind turbines will certainly be built in deeper and deeper waters at more exposed sites, and the Wavestar converter can follow this development thereby expanding into larger energy producing facilities.

The model predicts full load factors of 25 to 40 %, which is in agreement with expectations of what is achievable for wave energy converters. In comparison this factor for today's optimised offshore wind turbines is about 40 to 50 %.

The predicted efficiency is about 20 to 50 % in average with values in the higher range for optimised future devices, which seems reasonable. In comparison offshore turbines deliver up to about 80 % of the power extractable from the wind (Betz limit), at rated operating speed.

The energy production by future Wavestar machines has been investigated by using a model to predict the performance. The estimations are made for a 20-float machine with closely spaced floats in two rows with 10 floats in each row. For the 60-float machine the spacing and lay-out is not decided, as this will depend on the further optimization and cost optimization. As long as there are no full scale long-term real measurements available from a complete Wavestar WEC, such predictions has a large degree of uncertainty. However, to the best knowledge of the authors of this report, the provided model estimates are reliable and can be achieved in the future if a focussed R&D on the Wavestar concept is performed.

3   A brief look-back on the involvement of Aalborg University

Aalborg University has participated in the following previous Wavestar test campaigns. Among other subjects Aalborg University has been responsible for the setups, measurements, and reporting of power production performance.

Wavestar test campaigns

- 2001: "Wavestar Tusindben Machine". Wave basin tests at Aalborg University. Device with 20 floats, Ø20cm spheres. Mechanical PTO solution with ratchet mechanism and weight lifting system [1].
- 2004 to 2005 (three periods): "Wavestar Scale 1:40 Machine". Laboratory tests at Aalborg University, device with up to 40 floats. Variable float shape, size and weight. Mechanical PTO solution with ratchet mechanism and disk brake system. See [2] for a summary and list of further references.
- 2006 to 2011 (July 2006 to November 2011): "Wavestar Nissum Machine". Open sea trial in Nissum Bredning with more than 5 years of continuous operation. Grid connected device with 38 floats, Ø1m. Hydraulic PTO and single generator system. See e.g. [3] for conclusions and further references.
- 2011: "Wavestar Nissum Mini Hydraulic Machine". Open sea trials in Nissum Bredning with single float device, Ø1m. Grid connected hydraulic PTO with real time control. See [3] for summary and further references.
- 2013 (November 2013): "Wavestar Plymouth Device". Wave basin tests at Plymouth University, device with a single float Ø1m. Detailed tests regarding forces on bearings and pressures on float shell. Hydraulic PTO with real time control (the PTO system used previously for the "Wavestar Nissum Mini Hydraulic Machine") [4-6].
- 2009 to 2013 (September 2009 to September 2013): "Wavestar Hanstholm Machine". Open sea trial in the North Sea with 4 years of continuous operation. Grid connected device with 2 floats, Ø5m. Hydraulic PTO and individual generator systems [7-10].
- 2012-2016 (ongoing): "Wavestar Aalborg Wave Basin Linear Actuator Device". Wave basin tests at Aalborg University, device with 1 to 5 floats Ø25cm. Detailed tests regarding extreme forces, control strategies and power output in small waves. Magnetic PTO with linear electrical actuators and real time control. [6, 11-13]
- 2013-2016 (ongoing): "Wavestar PTO Test bench". Dry test of a full scale digital hydraulic PTO system at Aalborg University. Real time control with a hydraulic cylinder which simulates the motion of a single float. Size for use with a single Ø5m float. See [11] and [14] for a list of new references.

Wavestar numerical modelling

Besides experimental testing Aalborg University has also worked intensively on numerical methods to simulate the Wavestar WEC and to further develop and improve the concept. The numerical models have focussed on increase the power production by the following:

- Improvement in PTO efficiency in order to decrease losses in the conversion from mechanical energy collected by the float and into electricity delivered to the grid [11, 14, 17].
- Control strategies that focusses on increasing the electrical energy output [15, 18-20].
- Physical parameters (float shape, float arrangement, weight, inertia moment, ...) which leads to better performance and higher output [21, 22].

For more in-depth information about numerical models and tests with Wavestar, reference is given to the PhD-projects from Aalborg University by Rico Hansen [11], Anders Hedegaard Hansen [17], Andrew Zurkinden [12], Francesco Ferri [13], Morten Møller [6] and Simon Ambühl [23].

4   Methods for increasing the power production

The energy production of the Wavestar WEC can be enlarged by:

- **PTO efficiency**: Increase in Power Take Off efficiency
- **Control**: More optimal control strategy
- **Design**: Improved physical design by adjusting float geometry, weight, inertia moment...
- **Layout**: More efficient layout (arrangement of floats, gap between floats)

The energy production from the single devices can further be increased by:

- **Number of floats**: Devices with additional floats
- **Scale/size**: Larger machines by increase in float size – diameter and height
- **Site**: Placement at high energetic sites, possibly further offshore at higher water depth

In the following sections further detail is given.

4.1   PTO efficiency

The PTO efficiency for the current level of development is expected to be 70 % for the first Wavestar WEC [11, 17] by using a first version of a digital hydraulic PTO. This level has been validated by dry test of a full scale digital hydraulic PTO system at Aalborg University (AAU), for further details see Section 2. However, further development of the digital hydraulic PTO is expected to reach a level of 80 % in the near future (4 years). This level may further be increased to 90 % in about 5 years' time by utilising more advanced components such as the magnetic lead screw [24], the Wavespring technology [25], use of hydraulic Digital Displacement Pumps – DDP [11], etc. as indicated in Figure 1.

Conventional hydraulic PTO	Digital hydraulic PTO		New PTO technology

50 %	70 % (current)	80 % (near future)	90 % (far future)

Figure 1: Development of more efficient PTO from 50 % to 90 % efficiency. Pictures are from Wavestar at Hanstholm (left), full scale digital hydraulic PTO system at AAU (middle), and small-scale tests of a magnetic lead screw at AAU (right).

4.2   Control

The reference control model is the standard PI controller which includes a gain factor on the position and a gain factor on the velocity. The gain factors are kept constant in a sea-state, such that no adjustment is performed online wave to wave, but only variations by sea-state is taken into account over a 10 min average window of the past [27].

The development of control strategies that focusses on increasing the electrical energy output with online control (wave by wave) and automatic optimization has demonstrated significant improvements in production performance relative to the reference control [15, 18-20]. It has been shown and validated by model tests that the current known control strategies can provide up to 50% increase in energy than the reference PI control [26, 34-36], see example in Figure 2.
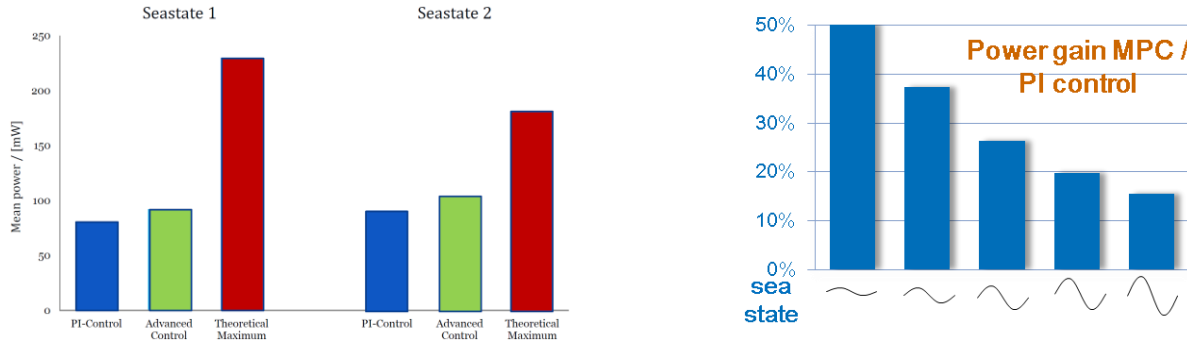
Figure 2: Results of control and power measurements on a single small scale Wavestar float in the wave basin at AAU. Left figure is from [35], right figure is from [26].

In the following cases it is expected that the control may provide an increase in power of 30 % (i.e. a control power gain factor = 1.3) in the near future (4 years). This level may further be increased to 60 % (i.e. a control power gain factor = 1.6) in about 5 years' time by utilising more advanced strategies.

4.3 Design

The dynamics of the float and arm system is strongly influencing the motion of the absorbers and the forces in play. The mass inertia moment and the hydrostatic stiffness are the most important parameters for the dynamic properties, and thereby the natural period of the dynamic system. A tuning of these properties to the wave climate where the Wavestar WECs will be located can amplify the motions and thereby increase the power production.

The shape of the Wavestar floats is also important as investigated numerically in [29] and experimentally in [30], see Figure 3. It was demonstrated that changing the shape of the floats may increase the power by 5% to 10 %.
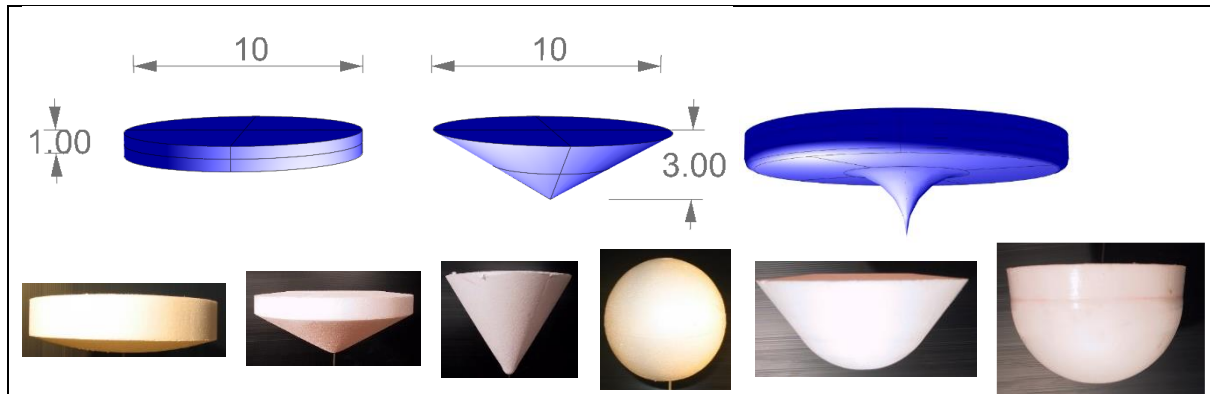
Figure 3: Some examples of Wavestar float shapes investigated in [29, 30].

The choice of orientation of the float arms relative to wave incidence is also of importance. As shown in [2] the horizontal wave forces contributes positively to the motion of the absorbers and thereby the power production when the wave incidence is θ = +90°, see Figure 4. In the laboratory tests increases by 10-20 % was realised for θ = +90°.
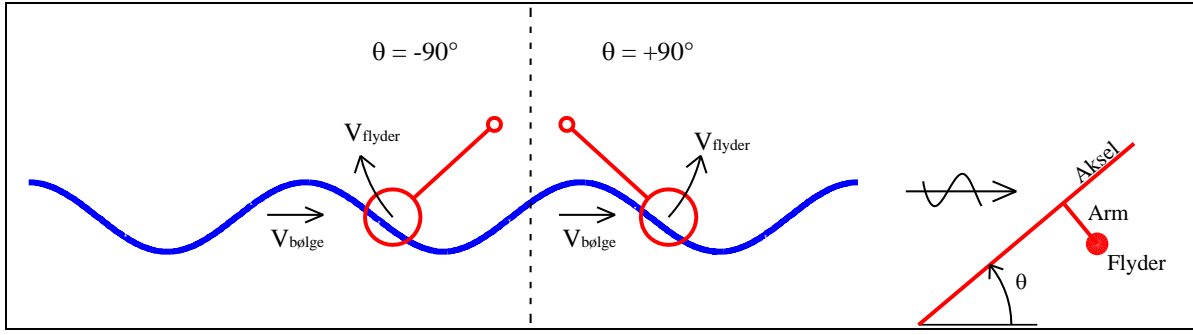
Figure 4: Sketch from [2] sowing the benefit in motion when θ = +90°.

4.4 Layout

The arrangement of the multiple floats in the array and the gap between floats are important and traditionally quantified by the array interaction factor also called the *q-factor*:

$$q = \frac{P}{NP^*}$$

, where *P* is the total power from the array, *N* is the number of devices and *P** is the power absorbed by an isolated device.

Normally the *q*-factor is less than 1 meaning that some shadowing effects will be present in the array, with typical values of about 0.72 for the full Wavestar WEC with 20 floats, but this value depends very much on the layout. As shown in the following section the *q*-factor is also very dependent on the number of floats. Figure 5 shows ideas to how the floats could be arranged in layouts in the future.

Larger gaps between the Wavestar floats reduces the shadowing effects and increases the *q*-factor as shown experimentally in [2] and numerically in [22], where increases in power production of more than 10 % was demonstrated for very large gaps (gaps of 1.4 times the float diameter).
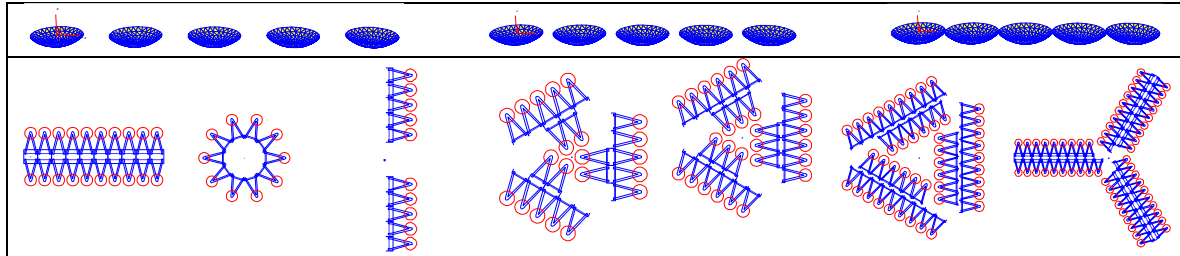
Figure 5: Layout of device. Upper part shows tree different gaps for a 5-float system [2, 22]. Lower part shows some different arrangement of floats. The reference case is the one on the left with 20 floats, 10 floats in each of the two lines.

4.5 Number of floats

A higher number of floats increases the total power production, but at the same time the shadowing effects also increases such that the power from the individual floats will decrease, i.e. the *q*-factor for the array will decrease for the machines with many floats such as the ones on the right in Figure 5. The price of the machine per float will decrease for machines with higher number of floats, so the price must be balanced with the production to find an optimal configuration. Nevertheless, as instal-lation costs, maintenance costs and foundation costs contribute with a large part of the total costs, machines with a significant amount of floats (say 20+) are presumably much more economical than machines with a single or just a very few floats.

In Appendix A estimations of the *q*-factor are given for some of the lay-outs shown in Figure 5. The calculated results are plotted as function of the number of floats in Figure 6. A simple formula has been fitted to the results as indicated by the blue line. The values by this line is used in the following by investigating the performance of a 20 float machine and a 60 float machine. The lay-out of the machine with 60 floats is not decided on.
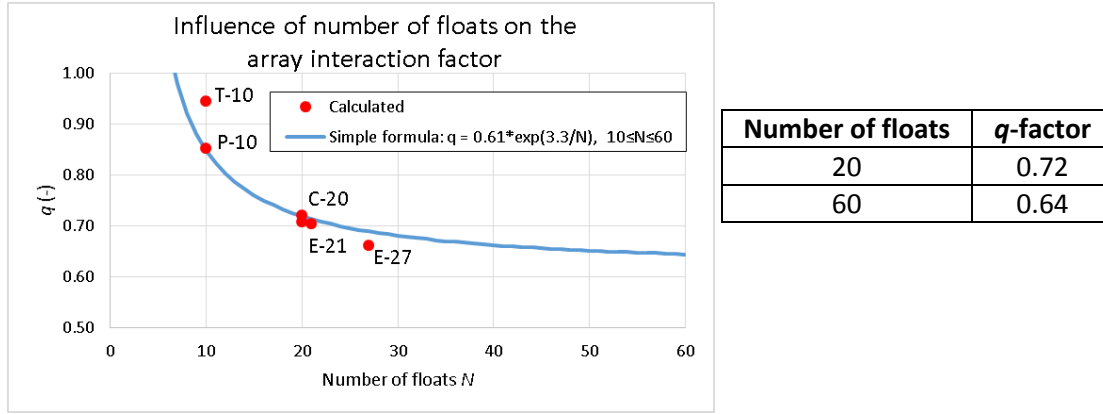
Figure 6: Number of floats and the array factor. Left figure shows calculated values from Appendix A together with a prediction formula. The predicted values corresponding to 20 and 60 floats are given in the table on the right.

It should be noted, that the calculated q-values from Appendix A are based on a very simple control strategy using optimal PI control gains from the single float case. Control strategies that maximises the total power production from a full machine with many floats, i.e. takes array interactions into account, may allow a higher production than simpler single-float strategies. As demonstrated in [21] a PI control with optimised array gains improved the yearly energy production of a three float array by 7.5 % as compared to control using simple single-float control gains. Higher q-factors may therefore be found for control strategies which are aware of the interactions.

4.6   Scale/size

Larger floats produces more power (to reasonable extend). The wave climate and power production may be scaled up by using the Froudes model law exactly in the same manner as done when scaling up small scale experiments [e.g. 1-3]. Froudes model law provides that power scales by $P_F = \lambda^{3.5} * P_M$ where λ is the scaling ratio, P_F is power at full scale and P_M is power at small scale. If $\lambda = 2$, i.e. a scaling of two (the machine is twice as big, the waves are twice as high...), the larger machine will produce $\lambda^{3.5} = 2^{3.5} = 11.3$ times more power. Larger machines are of course also more costly, and if they are not to be placed at a site with higher and longer waves, the benefit by going up in size may not be worth it. The size should therefore be optimized based on the site in question.

4.7   Site

Looking at European locations there is a very large spatial difference in the average offshore wind and wave resource, see Figure 7 and Figure 8. A site with a higher wave resource may allow an increase in the yearly production as demonstrated in the following sections. It should however be noted, that more exposed sites with a higher wave climate also normally have higher extreme environmental values, such as higher extreme wave heights for rare events as the 50-year value. In order for the structure to survive the more exposed conditions, the design at the exposed site will normally involve higher structural costs.
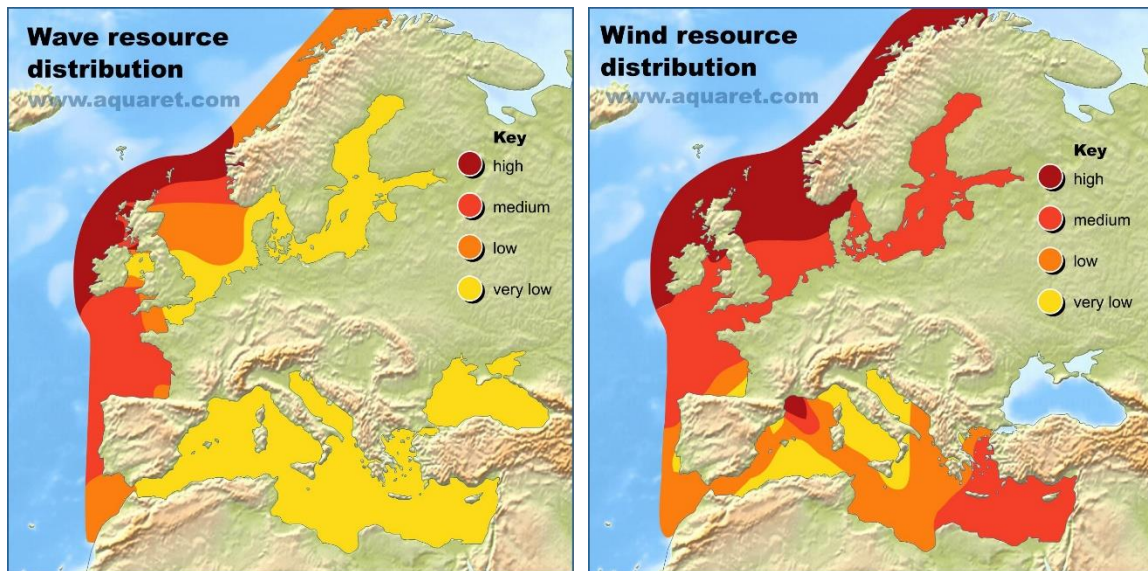
Figure 7: Wind and Wave Resource in Europe. Maps are from [31].

Figure 8: Wave Resource in Europe. Values are average wave power in "kW/m". Map is from [32].

5 Cases

11 cases are defined described by *Case A ...Case K* as indicated by the columns in Table 1, where *Case A* is the first machine which produces least power and *Case K* is a far future machine which is producing the most. The time frame for the cases is described in the row with perspective in years, meaning that machines could be installed in the given number of years, i.e. the time frame includes phases for research, development and construction. The reference case in the left column is the prototype in Hanstholm with two floats, diameter Ø5 m. The further development of the Wavestar machines may start by an optimization of the *Demonstrator* device with 20 floats, diameter Ø6 m, which is planned to be installed within 3 years in Belgium using funding from EU Horizon 2020 [33], as indicated in Table 1 by *Case A*, *B* and *C*. This could be followed in 5-6 years' time by building an optimised and new *Pre-commercial* or a high number of *Commercial* 20 float machines suitable for serial production (*Case D* and *E*). In 7 to 10 years' time the number of the floats on a single machine could further be increased (*Commercial 60 float Ø6, Case F, G,* and *H*), and the size of the machines and floats could be increased to a diameter of 8 m (*Commercial 60 float Ø8, Case I, J,* and *K*). During the development phases improvements are expected as described in Section 4. Improvements are in terms of power take off efficiency (level is raised gradually from 50 % to 90 %), control strategy (power level is raised first by a factor 1.3 and later by 1.6), and by design (power level is raised up to a factor 1.2). The total power gain factor is found by multiplying the control power gain and the design power gain, and as seen in the last row of Table 1 this factor is expected to raise up to a factor 1.9. It is also expected that it will be possible to operate the machines in more rough conditions, and therefore the storm protection wave height is expected to be increased over time to allow production to take place in higher waves.

Table 1: Details for the cases.

Case	Hanstholm	Demonstrator 20 float Ø6			(Pre-)commercial 20 float Ø6		Commercial 60 float Ø6			Commercial 60 float Ø8		
	Reference	A	B	C	D	E	F	G	H	I	J	K
Perspective	-	3 years	4 years	5 years	6 years	6 years	6 years	7 years	7 years	8 years	10 years	10 years
Float numbers	2	20	20	20	20	20	60	60	60	60	60	60
Float diameter (m)	5	6	6	6	6	6	6	6	6	8	8	8
Site characteristics	Hanstholm	Be	Be	Be	Fr	Fr	Fr	Fr	Fr2	Fr	UK	UK (100m)
PTO%	50%	70%	80%	90%	90%	90%	90%	90%	90%	90%	90%	90%
Power gain factor	1	1.0	1.3	1.6	1.6	1.9	1.6	1.9	1.9	1.9	1.9	1.9
Storm protection [m]	3.0	3.5	3.5	3.5	4.0	4.0	4.0	4.0	4.5	5.0	5.0	5.0
Min. PTO power [kW]	0	10	10	10	10	10	30	30	30	50	50	50
Max. PTO power [kW]	110	1000	1000	1000	2000	2000	4000	4000	4000	15000	15000	15000
Background consumption [kW]	-	10	10	10	20	20	50	50	50	100	100	100
Power gain details												
Control power gain	1	1	1.3	1.6	1.6	1.6	1.3	1.6	1.6	1.6	1.6	1.6
Design power gain	1	1	1	1	1	1.2	1.2	1.2	1.2	1.2	1.2	1.2
Total power gain factor	1.0	1.0	1.3	1.6	1.6	1.9	1.6	1.9	1.9	1.9	1.9	1.9

Site characteristics are described in Section 6 and 7, and power production characteristics (storm protection wave height, min/max PTO power and background consumption) is described in Section 8 and 9. Based on this the power performance estimations for the cases are given in Section 10.

The cases are further explained in the following:

Case A, B, C: Demonstrator with 20 float Ø6 m in Belgium
Case A is a device which may be build and installed in the near future (3 years) assisted by funding from the EU Horizon 2020 project [33]. Going through some of the rows in Table 1 it is seen that this device has 20 floats, 6 meter diameter, it will be installed at a Belgian site, it has a PTO efficiency of 70 %, and no expectations are included for gains in power performance (power gain factor = 1).

Case B is the same device as in *Case A*, but with a short further time of development the control is expected to increase the production by 30 % (control power gain = 1.3) and the PTO efficiency is expected to be increased to 80 %.

Case C is an even further developed version of the same device as in *Case A* where the control is increasing the production by 60 % (control power gain = 1.6) and the PTO efficiency is developed to reach a level of 90 %.

Case D, E: Pre-commercial or commercial machine with 20 float Ø6 m in France (or at similar site)
Case D is a further upgrade of the same machine, but now placed at a more energetic French site with storm protection at H_{m0} = 4.0. It is further rated at a maximum production of 2000 kW.

Case E is similar to *Case D* with the exception that a new design of the machine is introduced which is able to increase the production by 20 % (design power gain = 1.2). The design power gain is also included for all of the following cases.

Case F, G, H: Commercial machine with 60 float Ø6 m in France (or similar site)
Case F is a machine with additional floats (60 in total). As the control of so many floats are presumably more challenging the control power gain for this device is set to 1.3.

Case G is the same as *Case F* with the exception that the control power gain is now increased to 1.6.

Case H is the same as *Case G* with the exception that the storm protection wave height is increased to H_{m0} = 4.5 m, and the site is changed to a more exposed site in France.

Case I, J, K: Commercial machine with 60 float Ø8 m at different sites
Case I is similar to *Case G* with the exception that the machine is scaled up to have an increased float diameter of 8 m. Storm protection is increased to H_{m0} = 5.0 m, and machine capacity is enlarged.

Case J is placed at UK (EMEC site) in order to see the difference in production compared to the French site used for *Case I*.

Case K is placed by the UK West coast far offshore at 100 m water depth. A floating structure will probably be needed for this configuration.

6   Sites for case studies

Wave climates at six sites are considered, see Figure 9. The wave climates are increasing in how exposed the sites are, going from an average wave power of only 2.6 kW/m at the Roshage test site in Denmark where the Wavestar prototype was tested, and to a deep site offshore UK at 100 m water depth with 42.3 kW/m of available wave power.

Location	Site	Name
	1 North Sea, low depth near coast, h = 6 m, P_w = 2.6 kW/m.	DK - Roshage
	2 North Sea, high depth near coast, h = 33 m, P_w = 5.4 kW/m.	Be - Mermaid
	3 North Atlantic, high depth near coast, h = 29 m, P_w = 22.7 kW/m.	Fr - 2611
	4 North Atlantic, high depth near coast, h = 20 m, P_w = 36.6 kW/m.	Fr - 3268
	5 North Atlantic, high depth near coast, h = 50 m, P_w = 20.6 kW/m.	UK - EMEC
	6 North Atlantic, high depth offshore, h = 100 m, P_w = 42.3 kW/m.	UK - 100m

Figure 9: Wave climates considered in the case studies. Map on left is from [31], a cropped version of Figure 7. h is water depth, and P_w is the average available wave power.

6.1   Site 1, DK – Roshage

This site is of particular interest as this is where the Wavestar Hanstholm WEC was located in the North Sea in Denmark [7-10]. The WEC and the wave measurement device was located in shallow water and this is the reason for the rather low wave power at the location as described in the following. The WEC was placed by the side of the Roshage Pier and waves coming from Eastern directions did therefore not reach the converter, see Figure 10. As the WEC was often in shelter of the pier there was a relatively large percentage of the time with calm sea at the location of the WEC.

Waves coming from Western directions are reflected by the pier and in this case the waves by Wavestar are a mix of incoming and reflected waves

Waves coming from Eastern directions are reflected by the pier and therefore do not reach Wavestar
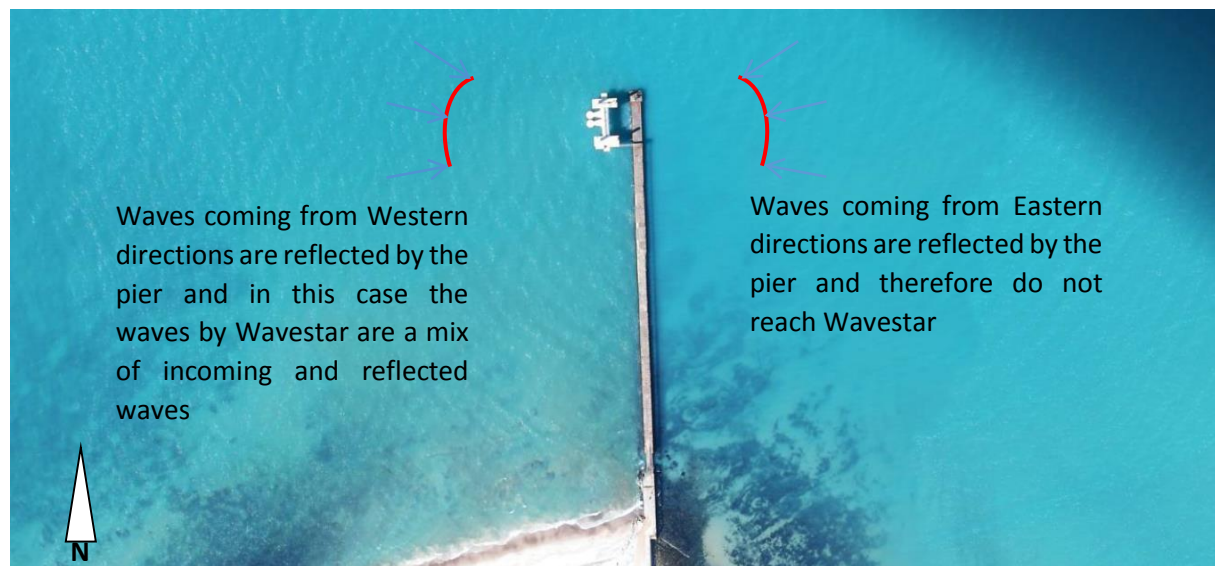
Figure 10: Position of Wavestar by Roshage with sketch of waves from Eastern and Western directions. Map is from google maps.

The bathymetry in the area and the low water depth at the location was causing substantial wave breaking when the significant wave height was exceeding approximately 2.0 m. A few measurements are available in the highest recorded sea states with significant wave heights slightly higher than 2.5 m, in which almost all the individual waves were breaking before or at the structure, see Figure 11.

The high waves are breaking in front of the WEC

Figure 11: Picture showing wave breaking in front of the WEC. The significant wave height by the time the picture was taken was 2.2 m.

The wave scatter diagram was based on wave measurements recorded by an ultrasonic wave sensor at the location. A complete one year of measurements covering a specific period (1 May 2011 to 1 May 2012) was used, as the measured power performance and wave data in this period was validated by the Danish electricity provider *Energinet.dk* [9]. The software package WaveLab developed at Aalborg University was used to analyse the measurements from the ultrasonic sensor [43].

6.2   Site 2, Be – Mermaid

The wave climate offshore Belgium is of interest as this is where the Wavestar demonstrator is planned to be placed inside one of the wind turbine parks, see Figure 12. The wave climate in the Belgian waters are described e.g. in [45, 46].

Mermaid site
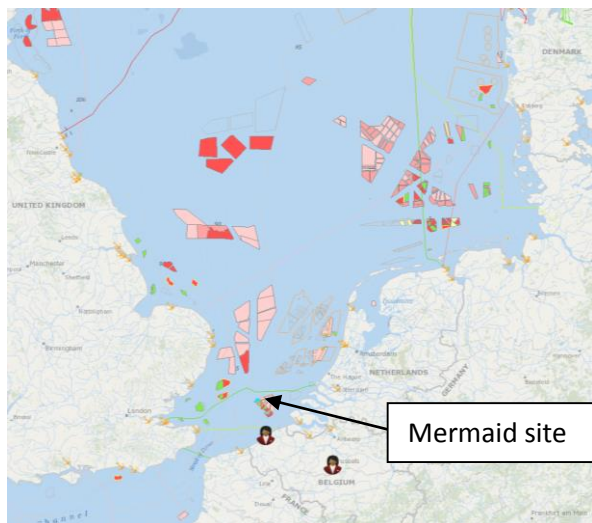
Figure 12: Offshore wind turbine parks in the Southern North Sea. Map is from [44].

6.3 Site 3, Fr – 2611

Renewable energy in France might become a big marked for Wavestar WECs in the future as the wave energy resource along the French coast is relatively high. Data from the ANEMOC database [47] has been used for the study, see Figure 13. The site no. 2611 is located approximately in the middle of the Bay of Biscay, and the wave climate at the location is approximately an average of what is found along the West facing coast. Therefore this particular site is chosen as representative for the case study.
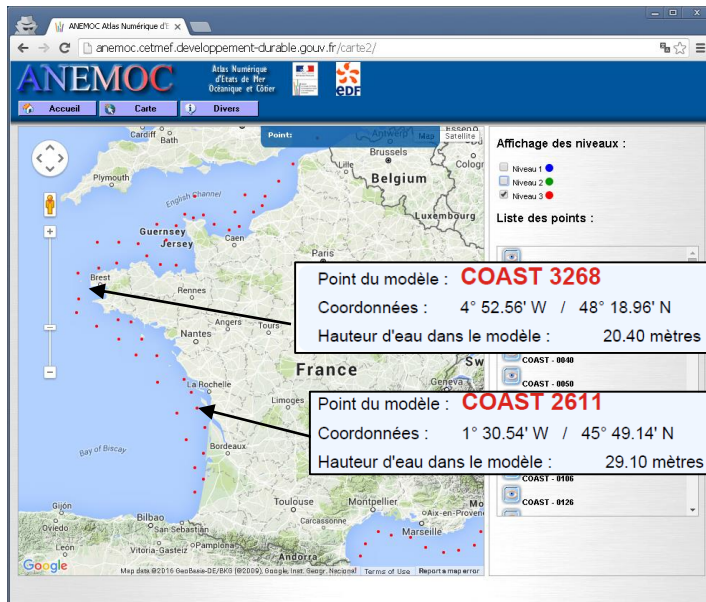
Figure 13: Anemoc database screen dump, dots are showing sites with validated data [47], highlight of site no 2611 and 3268.

6.4 Site 4, Fr – 3268

This site is selected from the Anemoc database as shown in Figure 13. It is located by Brest in the Northern part of the Bay of Biscay, and the wave climate at the location is relatively high. The scatter diagram for the site is shown in Figure 14.

Corrélogramme Hm0 / T02 - ANEMOC_COAST_3268 - annuel

Hm0 (m)	T02 (Secondes)																	Total
0	1	2	3	4	5	6	7	8	9	10	11	12	13	14	15	16	17	Total
0.5			0.32	3.34	4.04	3.79	1.37	0.62	0.03									13.51
1			0.83	34.00	38.58	37.21	31.43	16.50	4.45	0.93	0.17	0.06						164.18
1.5				17.35	65.53	38.08	30.76	29.58	19.43	9.39	2.73	0.61	0.18	0.01				213.66
2				0.92	39.94	42.48	23.36	19.60	16.99	14.20	7.53	2.18	0.49	0.14				167.82
2.5					7.94	38.83	20.78	14.95	12.05	9.31	8.16	3.79	0.91	0.23	0.06			117.02
3					0.40	16.47	23.28	14.05	10.35	7.77	6.25	5.51	1.98	0.75	0.06			86.87
3.5						1.40	18.94	14.56	9.50	5.57	5.07	3.81	2.21	1.02	0.18	0.02		62.29
4						0.10	7.40	15.14	9.54	5.26	3.78	3.85	2.14	0.93	0.25	0.08		48.48
4.5						0.00	0.70	10.07	10.13	5.50	3.43	2.67	1.91	0.81	0.30	0.06		35.57
5							0.05	3.12	8.99	6.06	2.77	1.90	1.33	1.13	0.39	0.05		25.79
5.5							0.01	0.47	5.44	6.51	3.45	2.32	1.43	0.84	0.26	0.04		20.78
6								0.07	2.01	4.66	3.30	2.32	1.44	0.50	0.26	0.01		14.58
6.5									0.26	2.67	2.92	2.35	1.16	0.48	0.20	0.03		10.06
7									0.08	1.07	2.26	1.78	1.07	0.51	0.22	0.09		7.08
7.5									0.01	0.25	1.37	1.76	1.04	0.59	0.25	0.07	0.01	5.35
8										0.02	0.35	1.30	1.39	0.80	0.51	0.12	0.05	4.54
8.5											0.00	0.09	0.47	0.45	0.71	0.44	0.25	2.42
Total			1.16	55.62	156.43	178.35	158.06	138.72	109.26	79.17	53.55	36.30	19.16	9.19	3.68	1.03	0.31	

Les valeurs du tableau sont exprimées en "pour mille (‰)" - Les valeurs 0.00 ‰ correspondent à des fréquences comprises entre 0 ‰ et 0.01 ‰ - Les case vides correspondent à des fréquences nulles.

Code des couleurs		
>= 10 ‰	>= 30 ‰	>= 50 ‰

Les intervalles sont à lire : "Borne inférieure incluse - borne supérieure exclue" (ex : 0.5 -> [0 - 0.5[ )   Page 1/1 - Edition du 28.03.07 - © CETMEF / EDF R&D-LNHE - Tous droits réservés

Figure 14: Scatter diagram for the site Fr-3268 from the Anemoc database.

6.5   Site 5, UK – EMEC

The EMEC wave test site is placed on the western edge of the Orkney mainland, at Billia Croo outside Stromness at Orkney in Scotland [37], see Figure 15 and Figure 16. Waves by the West coast of Scotland are fairly similar to the conditions by the EMEC wave test site.

Figure 15: EMEC location. The location is shown by bullet "North Atlantic Ocean" on right map. Maps are from google maps.

Figure 16: EMEC description. Map is from [37].

As seen in [38] and in Figure 17 the yearly average wave power offshore at the EMEC site is about 40 kW/m, whereas at 10 to 50m water depth the available wave power is about 20 to 25 kW/m.
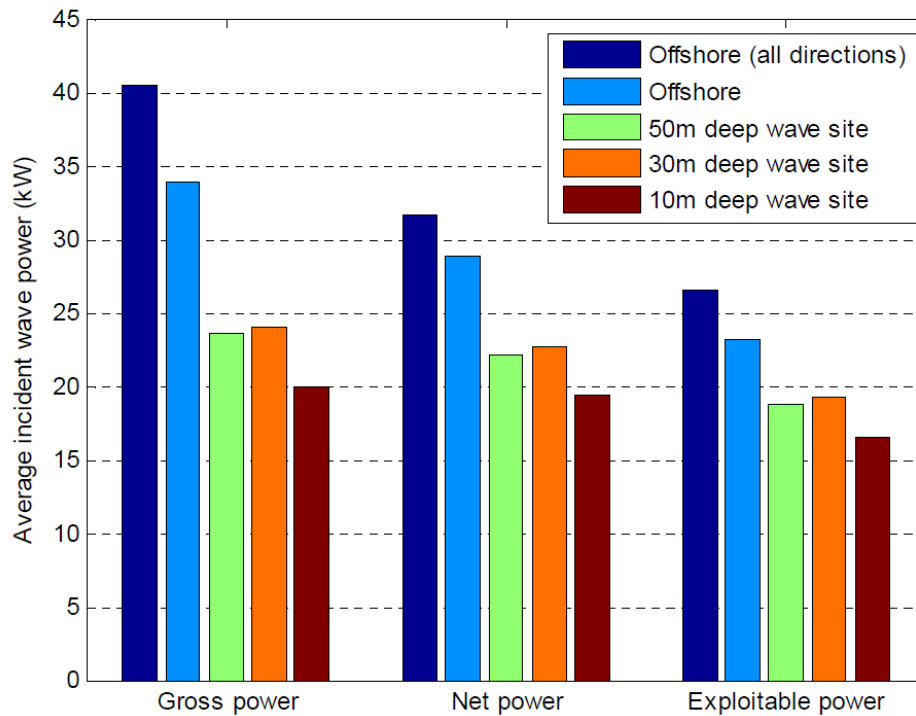
Figure 17: Wave energy resource at EMEC. Note that unit on y-axis should have been in [kW/m]. Figure is from [38].

The wave conditions at EMEC is given in the wave scatter diagram from [39] and [40], see Figure 18. The water depth is 50 m, 1-2 km from the coast, and the wave power is 21 kW/m. The energy content is roughly in agreement with the numbers given in Figure 17.

Table 18 - Joint probability diagram (H_s and T_z) for the EMEC location RP5OS 59,00°N;3,66°W (absolute numbers of occurrences, all directions, all year)

Hs \ Tz	<3	3,5	4,5	5,5	6,5	7,5	8,5	9,5	10,5	11,5	12,5	13,5	14,5	Sum	Tz ave	dP
0,25		2653	3618	1943	791	356	250	137	31	2				9781	4,89	0,02
0,75		2273	9363	5794	2063	734	182	85	40	2				20536	5,05	0,34
1,25		453	6484	6977	2946	1131	328	106	38		9	7	2	18481	5,48	0,93
1,75		130	2035	7652	2823	1029	352	139	21	0		5		14186	5,81	1,48
2,25			288	5405	3838	1081	319	184	66	9				11190	6,20	2,06
2,75			26	1135	5072	1135	234	137	52	17	2		2	7812	6,65	2,31
3,25			5	137	3278	2002	250	106	35	19	7			5839	7,01	2,54
3,75				14	713	2714	415	92	14	9	2			3973	7,49	2,46
4,25					57	1725	550	94	40	19	0	5	5	2495	7,88	2,09
4,75					7	430	861	118	26	14	5			1461	8,35	1,62
5,25						45	767	144	31	5				992	8,68	1,40
5,75						0	267	255	7	2	5			536	9,05	0,94
6,25					2	5	54	227	14	5				307	9,35	0,66
6,75						5	5	142	80	5				237	9,82	0,62
7,25								66	111		2			179	10,15	0,56
7,75								31	109	2	2			144	10,33	0,53
8,25								7	31	21				59	10,74	0,25
8,75									26	26				52	11,00	0,26
9,25									2	19	5			26	11,62	0,15
9,75										14	2			16	11,63	0,10
10,25										7	2			9	11,72	0,07
10,75											2			2	12,50	0,02
11,25											5			5	12,50	0,05
11,75														0		
Sum	0	5509	21819	29057	21590	12392	4834	2070	774	197	50	17	9	98318		21,46

Figure 18: EMEC conditions. Left: bathymetry [40, Figure 22]. Right: Wave scatter diagram [40, Table 18]. The location at 50 m depth where the scatter diagram is extracted is marked with a red circle on the left map.

The scatter diagram shown in the right table in Figure 18 is adjusted to give 100 % in total, hereby the scatter diagram going up to H_{m0} = 10.0 m given in

Table 6 in the following section is found.

6.6   Site 6, UK – 100 m

Further offshore at higher water depths the wave power is significantly higher than close to the coast, see Figure 19. In the future it may be chosen to make floating Wavestar WECs suitable for such exposed locations. A site at 100 m depth is investigated to give an indication about the level of production that could be expected at such a site.
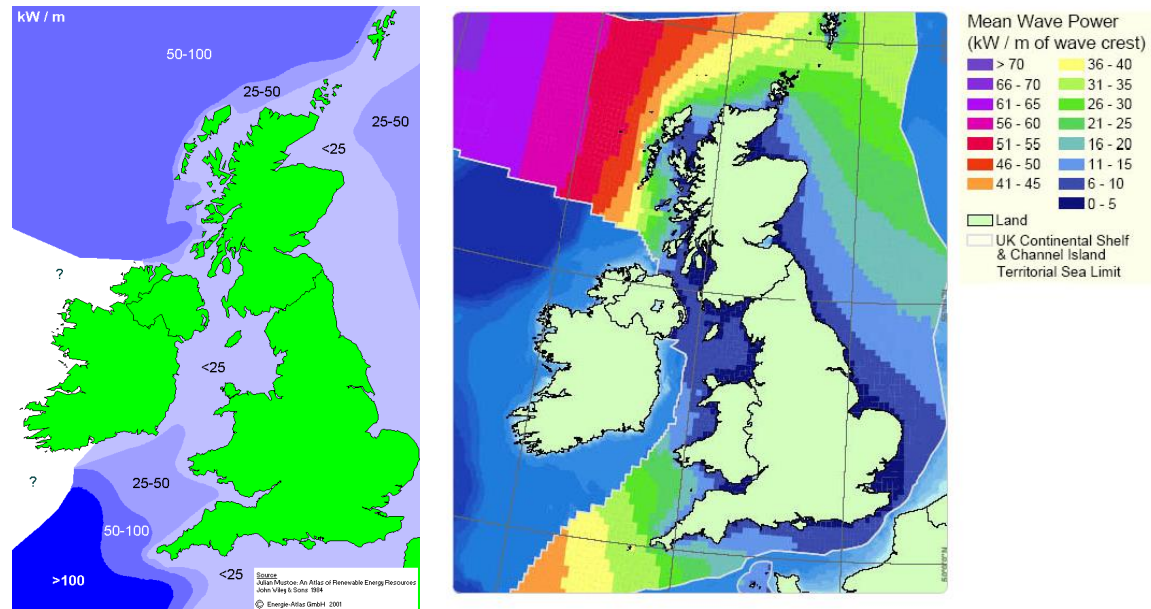
Figure 19: Wave energy resource around UK. Wave power is growing with increasing distance to shore. Maps are from [32].

An overview of wave and wind measurements around UK can be found in [41], see Figure 20. In the following focus is on the waves by the West coast of Scotland, so on waves in the area by the green arrow in Figure 20.
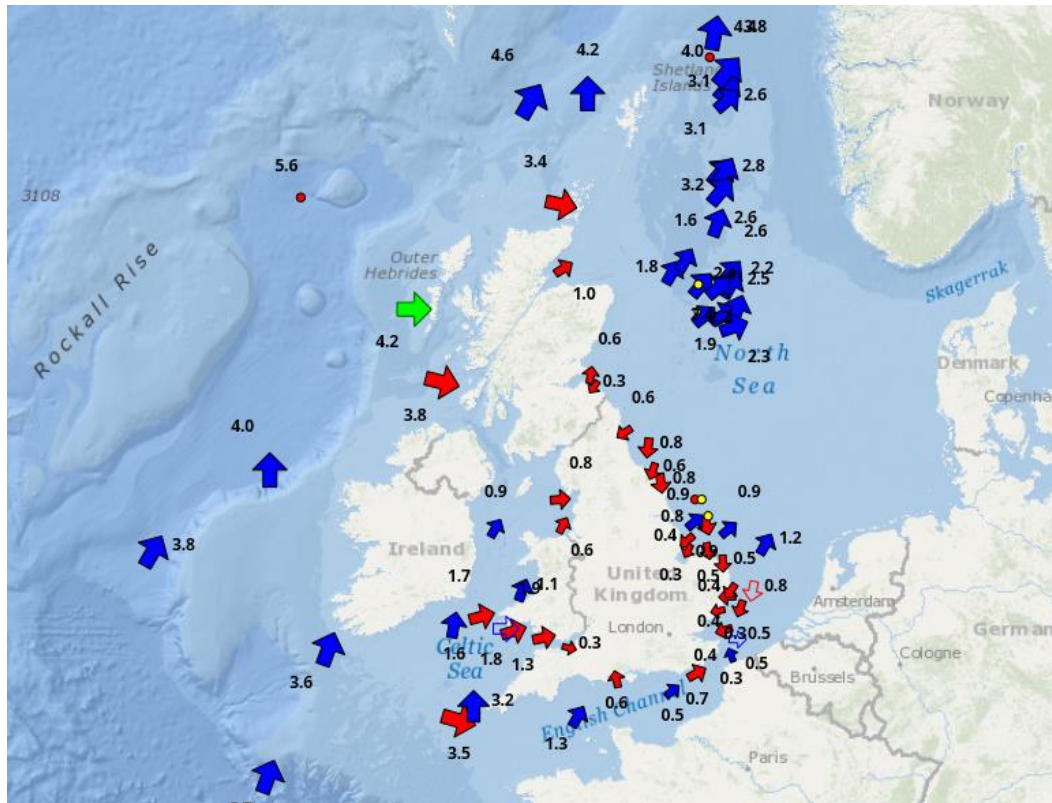
Figure 20: Overview of wave and wind measurements around UK. Map is a snapshot from [41] 2015-10-23. Red arrows indicates wave direction, blue wind direction, the green indicates the buoy used for the wave climate in the present study.

Significant wave height and mean wave period data, collected over a year, by the float indicated by the green arrow in Figure 20 at 100 m depth, has been used. The data has been obtained from the Wavenet database [41]. The complete scatter diagram going up to H_{m0} = 10.0 m is given in Table 7 in the following section.

7   Wave scatter diagrams for the six sites

Scatter diagrams for the six sites introduced in Figure 9 in the previous section are given below in Table 2 to 7.

Table 2: Wave scatter diagram for site 1 "DK-Roshage". Coloured values are in % with total = 100 %.

	Hm0 [m]	Hm0 [m]	Wave period T0,2 [s]																All		T02 [s]	dP [kW/m]
Site			0-1	1-2	2-3	3-4	4-5	5-6	6-7	7-8	8-9	9-10	10-11	11-12	12-13	13-14	14-15	15-16				
			0.5	1.5	2.5	3.5	4.5	5.5	6.5	7.5	8.5	9.5	10.5	11.5	12.5	13.5	14.5	15.5				
Denmark (Roshage - may'11-'12)	0.0 - 0.5	0.25	0.00	0.00	7.88	13.07	5.42	0.93	0.14	0.02	0.00	0.00	0.00	0.00	0.00	0.00	0.00	0.00	27.45		3.50	0.03
Depth [m]	0.5 - 1.0	0.75	0.00	0.00	2.59	23.38	11.56	2.39	0.15	0.00	0.00	0.00	0.00	0.00	0.00	0.00	0.00	0.00	40.06		3.85	0.49
5	1.0 - 1.5	1.25	0.00	0.00	0.00	8.61	8.48	0.38	0.00	0.00	0.00	0.00	0.00	0.00	0.00	0.00	0.00	0.00	17.48		4.03	0.62
T0,2 avg [s]	1.5 - 2.0	1.75	0.00	0.00	0.00	0.97	9.12	0.31	0.00	0.00	0.00	0.00	0.00	0.00	0.00	0.00	0.00	0.00	10.40		4.44	0.79
3.88	2.0 - 2.5	2.25	0.00	0.00	0.00	0.02	3.87	0.13	0.00	0.00	0.00	0.00	0.00	0.00	0.00	0.00	0.00	0.00	4.03		4.53	0.52
Hm0 avg [m]	2.5 - 3.0	2.75	0.00	0.00	0.00	0.00	0.57	0.01	0.00	0.00	0.00	0.00	0.00	0.00	0.00	0.00	0.00	0.00	0.58		4.51	0.11
0.88	3.0 - 3.5	3.25	0.00	0.00	0.00	0.00	0.00	0.00	0.00	0.00	0.00	0.00	0.00	0.00	0.00	0.00	0.00	0.00	0.00			
Pw avg [kW/m]	3.5 - 4.0	3.75	0.00	0.00	0.00	0.00	0.00	0.00	0.00	0.00	0.00	0.00	0.00	0.00	0.00	0.00	0.00	0.00	0.00			
2.6	4.0 - 4.5	4.25	0.00	0.00	0.00	0.00	0.00	0.00	0.00	0.00	0.00	0.00	0.00	0.00	0.00	0.00	0.00	0.00	0.00			
	4.5 - 5.0	4.75	0.00	0.00	0.00	0.00	0.00	0.00	0.00	0.00	0.00	0.00	0.00	0.00	0.00	0.00	0.00	0.00	0.00			
	All		0.00	0.00	10.46	46.05	39.02	4.15	0.29	0.02	0.00	0.00	0.00	0.00	0.00	0.00	0.00	0.00	100.00		3.88	2.6

Table 3: Wave scatter diagram for site 2 "Be-Mermaid". Coloured values are in % with total = 100 %.

|	Hm0 [m]	Hm0 [m]	Wave period T0,2 [s]																All		T02 [s]	dP [kW/m]
Site			0-1	1-2	2-3	3-4	4-5	5-6	6-7	7-8	8-9	9-10	10-11	11-12	12-13	13-14	14-15	15-16				
			0.5	1.5	2.5	3.5	4.5	5.5	6.5	7.5	8.5	9.5	10.5	11.5	12.5	13.5	14.5	15.5				
Belgium (Mermaid)	0.0 - 0.5	0.25	0.00	0.00	0.00	10.30	3.00	0.00	0.00	0.00	0.00	0.00	0.00	0.00	0.00	0.00	0.00	0.00	13.30		3.73	0.02
Depth [m]	0.5 - 1.0	0.75	0.00	0.00	0.00	18.60	11.70	0.00	0.00	0.00	0.00	0.00	0.00	0.00	0.00	0.00	0.00	0.00	30.30		3.89	0.37
33	1.0 - 1.5	1.25	0.00	0.00	0.00	6.60	16.50	4.10	0.00	0.00	0.00	0.00	0.00	0.00	0.00	0.00	0.00	0.00	27.20		4.41	1.05
T0,2 avg [s]	1.5 - 2.0	1.75	0.00	0.00	0.00	0.00	10.60	5.70	0.00	0.00	0.00	0.00	0.00	0.00	0.00	0.00	0.00	0.00	16.30		4.85	1.35
4.34	2.0 - 2.5	2.25	0.00	0.00	0.00	0.00	3.10	4.00	0.00	0.00	0.00	0.00	0.00	0.00	0.00	0.00	0.00	0.00	7.10		5.06	1.02
Hm0 avg [m]	2.5 - 3.0	2.75	0.00	0.00	0.00	0.00	0.00	3.20	0.00	0.00	0.00	0.00	0.00	0.00	0.00	0.00	0.00	0.00	3.20		5.50	0.74
1.22	3.0 - 3.5	3.25	0.00	0.00	0.00	0.00	0.00	2.60	0.00	0.00	0.00	0.00	0.00	0.00	0.00	0.00	0.00	0.00	2.60		5.50	0.84
Pw avg [kW/m]	3.5 - 4.0	3.75	0.00	0.00	0.00	0.00	0.00	0.00	0.00	0.00	0.00	0.00	0.00	0.00	0.00	0.00	0.00	0.00	0.00			
5.4	4.0 - 4.5	4.25	0.00	0.00	0.00	0.00	0.00	0.00	0.00	0.00	0.00	0.00	0.00	0.00	0.00	0.00	0.00	0.00	0.00			
	4.5 - 5.0	4.75	0.00	0.00	0.00	0.00	0.00	0.00	0.00	0.00	0.00	0.00	0.00	0.00	0.00	0.00	0.00	0.00	0.00			
	All		0.00	0.00	0.00	35.50	44.90	19.60	0.00	0.00	0.00	0.00	0.00	0.00	0.00	0.00	0.00	0.00	100.00		4.34	5.4

*Table 4: Wave scatter diagram for site 3 "**Fr-2611**". Coloured values are in % with total = 100 %.*

Site	Hm0 [m]	Hm0 [m]	0-1	1-2	2-3	3-4	4-5	5-6	6-7	7-8	8-9	9-10	10-11	11-12	12-13	13-14	14-15	15-16	All	T02 [s]	dP [kW/m]
			0.5	1.5	2.5	3.5	4.5	5.5	6.5	7.5	8.5	9.5	10.5	11.5	12.5	13.5	14.5	15.5			
France - 2611	0.0 - 0.5	0.25	0.00	0.00	0.27	1.31	1.96	2.57	2.91	2.41	1.64	0.90	0.53	0.25	0.07	0.03	0.01	0.00	14.85	6.57	0.03
Depth [m]	0.5 - 1.0	0.75	0.00	0.00	0.27	1.31	1.96	2.57	2.91	2.41	1.64	0.90	0.53	0.25	0.07	0.03	0.01	0.00	14.85	6.57	0.31
29.1	1.0 - 1.5	1.25	0.00	0.00	0.00	0.28	2.32	3.37	2.98	3.09	2.97	2.40	1.54	0.65	0.25	0.05	0.02	0.00	19.90	7.44	1.30
T0,2 avg [s]	1.5 - 2.0	1.75	0.00	0.00	0.00	0.28	2.32	3.37	2.98	3.09	2.97	2.40	1.54	0.65	0.25	0.05	0.02	0.00	19.90	7.44	2.54
7.55	2.0 - 2.5	2.25	0.00	0.00	0.00	0.00	0.07	1.27	1.82	1.31	1.13	1.09	1.01	0.76	0.23	0.06	0.01	0.01	8.76	8.24	2.05
Hm0 avg [m]	2.5 - 3.0	2.75	0.00	0.00	0.00	0.00	0.07	1.27	1.82	1.31	1.13	1.09	1.01	0.76	0.23	0.06	0.01	0.01	8.76	8.24	3.06
1.73	3.0 - 3.5	3.25	0.00	0.00	0.00	0.00	0.00	0.03	0.67	0.94	0.62	0.44	0.34	0.28	0.18	0.06	0.03	0.01	3.60	8.75	1.86
Pw avg [kW/m]	3.5 - 4.0	3.75	0.00	0.00	0.00	0.00	0.00	0.03	0.67	0.94	0.62	0.44	0.34	0.28	0.18	0.06	0.03	0.01	3.60	8.75	2.48
22.7	4.0 - 4.5	4.25	0.00	0.00	0.00	0.00	0.00	0.00	0.02	0.34	0.51	0.34	0.18	0.11	0.10	0.05	0.01	0.00	1.66	9.34	1.57
	4.5 - 5.0	4.75	0.00	0.00	0.00	0.00	0.00	0.00	0.02	0.34	0.51	0.34	0.18	0.11	0.10	0.05	0.01	0.00	1.66	9.34	1.96
	5.0 - 5.5	5.25	0.00	0.00	0.00	0.00	0.00	0.00	0.00	0.01	0.17	0.22	0.17	0.07	0.02	0.01	0.00	0.00	0.68	9.89	1.04
	5.5 - 6.0	5.75	0.00	0.00	0.00	0.00	0.00	0.00	0.00	0.01	0.17	0.22	0.17	0.07	0.02	0.01	0.00	0.00	0.68	9.89	1.24
	6.0 - 6.5	6.25	0.00	0.00	0.00	0.00	0.00	0.00	0.00	0.00	0.01	0.09	0.12	0.06	0.02	0.01	0.00	0.00	0.30	10.59	0.70
	6.5 - 7.0	6.75	0.00	0.00	0.00	0.00	0.00	0.00	0.00	0.00	0.01	0.09	0.12	0.06	0.02	0.01	0.00	0.00	0.30	10.59	0.82
	7.0 - 7.5	7.25	0.00	0.00	0.00	0.00	0.00	0.00	0.00	0.00	0.00	0.01	0.04	0.06	0.02	0.00	0.00	0.00	0.13	11.37	0.45
	7.5 - 8.0	7.75	0.00	0.00	0.00	0.00	0.00	0.00	0.00	0.00	0.00	0.01	0.04	0.06	0.02	0.00	0.00	0.00	0.13	11.37	0.51
	8.0 - 8.5	8.25	0.00	0.00	0.00	0.00	0.00	0.00	0.00	0.00	0.00	0.00	0.01	0.02	0.02	0.01	0.00	0.00	0.05	12.10	0.22
	8.5 - 9.0	8.75	0.00	0.00	0.00	0.00	0.00	0.00	0.00	0.00	0.00	0.00	0.01	0.02	0.02	0.01	0.00	0.00	0.05	12.10	0.24
	9.0 - 9.5	9.25	0.00	0.00	0.00	0.00	0.00	0.00	0.00	0.00	0.00	0.00	0.00	0.01	0.01	0.01	0.00	0.00	0.03	12.66	0.17
	9.5 - 10.0	9.75	0.00	0.00	0.00	0.00	0.00	0.00	0.00	0.00	0.00	0.00	0.00	0.01	0.01	0.01	0.00	0.00	0.03	12.66	0.19
	All		0.00	0.00	0.54	3.17	8.71	14.46	16.80	16.21	14.09	10.93	7.87	4.52	1.83	0.57	0.19	0.07	99.94	7.55	22.7

*Table 5: Wave scatter diagram for site 4 "**Fr-3268**". Coloured values are in % with total = 100 %.*

Site	Hm0 [m]	Hm0 [m]	0-1	1-2	2-3	3-4	4-5	5-6	6-7	7-8	8-9	9-10	10-11	11-12	12-13	13-14	14-15	15-16	All	T02 [s]	dP [kW/m]
			0.5	1.5	2.5	3.5	4.5	5.5	6.5	7.5	8.5	9.5	10.5	11.5	12.5	13.5	14.5	15.5			
France - 3268	0.0 - 0.5	0.25	0.00	0.00	0.03	0.33	0.40	0.38	0.14	0.06	0.00	0.00	0.00	0.00	0.00	0.00	0.00	0.00	1.35	4.84	0.00
Depth [m]	0.5 - 1.0	0.75	0.00	0.00	0.08	3.40	3.86	3.72	3.14	1.65	0.45	0.09	0.02	0.01	0.00	0.00	0.00	0.00	16.42	5.34	0.28
20.4	1.0 - 1.5	1.25	0.00	0.00	0.00	1.74	6.55	3.81	3.08	2.96	1.94	0.94	0.27	0.06	0.02	0.00	0.00	0.00	21.37	5.99	1.12
T0,2 avg [s]	1.5 - 2.0	1.75	0.00	0.00	0.00	0.09	3.99	4.25	2.34	1.70	1.42	0.75	0.22	0.05	0.01	0.00	0.00	0.00	16.78	6.60	1.90
7.05	2.0 - 2.5	2.25	0.00	0.00	0.00	0.00	0.79	3.88	2.08	1.50	1.21	0.93	0.82	0.38	0.09	0.02	0.01	0.00	11.70	7.11	2.36
Hm0 avg [m]	2.5 - 3.0	2.75	0.00	0.00	0.00	0.00	0.04	1.65	2.33	1.41	1.04	0.78	0.63	0.55	0.20	0.08	0.01	0.00	8.69	7.78	2.86
2.24	3.0 - 3.5	3.25	0.00	0.00	0.00	0.00	0.00	0.14	1.89	1.46	0.95	0.56	0.51	0.38	0.22	0.10	0.02	0.00	6.23	8.27	3.04
Pw avg [kW/m]	3.5 - 4.0	3.75	0.00	0.00	0.00	0.00	0.00	0.01	0.74	1.51	0.95	0.53	0.38	0.39	0.21	0.09	0.03	0.01	4.85	8.69	3.32
36.6	4.0 - 4.5	4.25	0.00	0.00	0.00	0.00	0.00	0.00	0.07	1.01	1.01	0.55	0.34	0.27	0.19	0.08	0.03	0.01	3.56	9.14	3.29
	4.5 - 5.0	4.75	0.00	0.00	0.00	0.00	0.00	0.00	0.01	0.31	0.90	0.61	0.28	0.19	0.13	0.11	0.04	0.01	2.58	9.58	3.12
	5.0 - 5.5	5.25	0.00	0.00	0.00	0.00	0.00	0.00	0.00	0.05	0.54	0.65	0.35	0.23	0.14	0.08	0.03	0.00	2.08	10.02	3.21
	5.5 - 6.0	5.75	0.00	0.00	0.00	0.00	0.00	0.00	0.00	0.01	0.20	0.47	0.33	0.23	0.14	0.05	0.03	0.00	1.46	10.42	2.81
	6.0 - 6.5	6.25	0.00	0.00	0.00	0.00	0.00	0.00	0.00	0.00	0.03	0.27	0.29	0.24	0.12	0.05	0.02	0.00	1.01	10.88	2.40
	6.5 - 7.0	6.75	0.00	0.00	0.00	0.00	0.00	0.00	0.00	0.00	0.01	0.11	0.23	0.18	0.11	0.05	0.02	0.01	0.71	11.28	2.04
	7.0 - 7.5	7.25	0.00	0.00	0.00	0.00	0.00	0.00	0.00	0.00	0.00	0.03	0.14	0.18	0.10	0.06	0.03	0.01	0.53	11.75	1.85
	7.5 - 8.0	7.75	0.00	0.00	0.00	0.00	0.00	0.00	0.00	0.00	0.00	0.00	0.04	0.13	0.14	0.08	0.05	0.01	0.45	12.53	1.89
	8.0 - 8.5	8.25	0.00	0.00	0.00	0.00	0.00	0.00	0.00	0.00	0.00	0.00	0.00	0.01	0.05	0.05	0.07	0.04	0.22	13.94	1.15
	8.5 - 9.0	8.75	0.00	0.00	0.00	0.00	0.00	0.00	0.00	0.00	0.00	0.00	0.00	0.00	0.00	0.00	0.00	0.00	0.00		
	9.0 - 9.5	9.25	0.00	0.00	0.00	0.00	0.00	0.00	0.00	0.00	0.00	0.00	0.00	0.00	0.00	0.00	0.00	0.00	0.00		
	9.5 - 10.0	9.75	0.00	0.00	0.00	0.00	0.00	0.00	0.00	0.00	0.00	0.00	0.00	0.00	0.00	0.00	0.00	0.00	0.00		
	All		0.00	0.00	0.12	5.56	15.64	17.84	15.81	13.87	10.93	7.92	5.35	3.63	1.92	0.92	0.37	0.10	99.96	7.05	36.6

*Table 6: Wave scatter diagram for site 5 "**UK-EMEC**". Coloured values are in % with total = 100 %.*

Site: UK (EMEC) — Depth [m]: 50 — T0,2 avg [s]: 5.93 — Hm0 avg [m]: 1.83 — Pw avg [kW/m]: 20.6

Hm0 [m]	Hm0 [m]	0-1	1-2	2-3	3-4	4-5	5-6	6-7	7-8	8-9	9-10	10-11	11-12	12-13	13-14	14-15	15-16	All	T02 [s]	dP [kW/m]
		0.5	1.5	2.5	3.5	4.5	5.5	6.5	7.5	8.5	9.5	10.5	11.5	12.5	13.5	14.5	15.5			
0.0 - 0.5	0.25	0.00	0.00	0.00	2.70	3.68	1.98	0.80	0.36	0.25	0.14	0.03	0.00	0.00	0.00	0.00	0.00	9.95	4.89	0.02
0.5 - 1.0	0.75	0.00	0.00	0.00	2.31	9.52	5.89	2.10	0.75	0.19	0.09	0.04	0.00	0.00	0.00	0.00	0.00	20.89	5.05	0.33
1.0 - 1.5	1.25	0.00	0.00	0.00	0.46	6.59	7.10	3.00	1.15	0.33	0.11	0.04	0.00	0.01	0.01	0.00	0.00	18.80	5.48	0.90
1.5 - 2.0	1.75	0.00	0.00	0.00	0.13	2.07	7.78	2.87	1.05	0.36	0.14	0.02	0.00	0.00	0.01	0.00	0.00	14.43	5.81	1.44
2.0 - 2.5	2.25	0.00	0.00	0.00	0.00	0.29	5.50	3.90	1.10	0.32	0.19	0.07	0.01	0.00	0.00	0.00	0.00	11.38	6.20	2.00
2.5 - 3.0	2.75	0.00	0.00	0.00	0.00	0.03	1.15	5.16	1.15	0.24	0.14	0.05	0.02	0.00	0.00	0.00	0.00	7.95	6.65	2.23
3.0 - 3.5	3.25	0.00	0.00	0.00	0.00	0.01	0.14	3.33	2.04	0.25	0.11	0.04	0.02	0.01	0.00	0.00	0.00	5.94	7.01	2.46
3.5 - 4.0	3.75	0.00	0.00	0.00	0.00	0.00	0.01	0.73	2.76	0.42	0.09	0.01	0.01	0.00	0.00	0.00	0.00	4.04	7.49	2.38
4.0 - 4.5	4.25	0.00	0.00	0.00	0.00	0.00	0.00	0.06	1.75	0.56	0.10	0.04	0.02	0.00	0.01	0.01	0.00	2.54	7.88	2.02
4.5 - 5.0	4.75	0.00	0.00	0.00	0.00	0.00	0.00	0.01	0.44	0.88	0.12	0.03	0.01	0.01	0.00	0.00	0.00	1.49	8.35	1.57
5.0 - 5.5	5.25	0.00	0.00	0.00	0.00	0.00	0.00	0.00	0.05	0.78	0.15	0.03	0.01	0.00	0.00	0.00	0.00	1.01	8.68	1.35
5.5 - 6.0	5.75	0.00	0.00	0.00	0.00	0.00	0.00	0.00	0.00	0.27	0.26	0.01	0.00	0.01	0.00	0.00	0.00	0.55	9.05	0.91
6.0 - 6.5	6.25	0.00	0.00	0.00	0.00	0.00	0.00	0.00	0.01	0.05	0.23	0.01	0.01	0.00	0.00	0.00	0.00	0.31	9.35	0.64
6.5 - 7.0	6.75	0.00	0.00	0.00	0.00	0.00	0.00	0.00	0.00	0.01	0.14	0.08	0.01	0.00	0.00	0.00	0.00	0.24	9.82	0.60
7.0 - 7.5	7.25	0.00	0.00	0.00	0.00	0.00	0.00	0.00	0.00	0.00	0.07	0.11	0.00	0.00	0.00	0.00	0.00	0.18	10.15	0.54
7.5 - 8.0	7.75	0.00	0.00	0.00	0.00	0.00	0.00	0.00	0.00	0.00	0.03	0.11	0.00	0.00	0.00	0.00	0.00	0.15	10.33	0.51
8.0 - 8.5	8.25	0.00	0.00	0.00	0.00	0.00	0.00	0.00	0.00	0.00	0.01	0.03	0.02	0.00	0.00	0.00	0.00	0.06	10.74	0.25
8.5 - 9.0	8.75	0.00	0.00	0.00	0.00	0.00	0.00	0.00	0.00	0.00	0.00	0.03	0.03	0.00	0.00	0.00	0.00	0.05	11.00	0.25
9.0 - 9.5	9.25	0.00	0.00	0.00	0.00	0.00	0.00	0.00	0.00	0.00	0.00	0.02	0.01	0.00	0.00	0.00	0.00	0.03	11.62	0.15
9.5 - 10.0	9.75	0.00	0.00	0.00	0.00	0.00	0.00	0.00	0.00	0.00	0.00	0.01	0.00	0.00	0.00	0.00	0.00	0.02	11.62	0.10
All		0.00	0.00	0.00	5.60	22.19	29.55	21.96	12.60	4.92	2.11	0.79	0.19	0.04	0.02	0.01	0.00	99.98	5.93	20.6

*Table 7: Wave scatter diagram for site 6 "**UK-100m**". Coloured values are in % with total = 100 %.*

Site: UK (100m) — Depth [m]: 100 — T0,2 avg [s]: 6.60 — Hm0 avg [m]: 2.76 — Pw avg [kW/m]: 42.3

Hm0 [m]	Hm0 [m]	0-1	1-2	2-3	3-4	4-5	5-6	6-7	7-8	8-9	9-10	10-11	11-12	12-13	13-14	14-15	15-16	All	T02 [s]	dP [kW/m]
		0.5	1.5	2.5	3.5	4.5	5.5	6.5	7.5	8.5	9.5	10.5	11.5	12.5	13.5	14.5	15.5			
0.0 - 0.5	0.25	0.00	0.00	0.00	0.25	0.43	0.01	0.00	0.00	0.00	0.00	0.00	0.00	0.00	0.00	0.00	0.00	0.69	4.15	0.00
0.5 - 1.0	0.75	0.00	0.00	0.00	2.00	2.38	1.57	0.65	0.13	0.03	0.01	0.00	0.00	0.00	0.00	0.00	0.00	6.76	4.71	0.10
1.0 - 1.5	1.25	0.00	0.00	0.00	1.21	3.95	4.56	1.40	0.64	0.17	0.06	0.00	0.00	0.00	0.00	0.00	0.00	12.00	5.26	0.55
1.5 - 2.0	1.75	0.00	0.00	0.00	0.06	2.85	6.14	3.02	1.65	0.87	0.31	0.01	0.00	0.00	0.00	0.00	0.00	14.91	5.99	1.53
2.0 - 2.5	2.25	0.00	0.00	0.00	0.00	0.37	6.34	3.98	2.20	0.74	0.35	0.13	0.02	0.00	0.00	0.00	0.00	14.12	6.38	2.55
2.5 - 3.0	2.75	0.00	0.00	0.00	0.00	0.01	4.68	5.85	2.36	1.27	0.34	0.05	0.01	0.00	0.00	0.00	0.00	14.55	6.60	4.06
3.0 - 3.5	3.25	0.00	0.00	0.00	0.00	0.00	1.21	5.43	2.53	1.36	0.58	0.07	0.04	0.00	0.00	0.00	0.00	11.21	7.06	4.67
3.5 - 4.0	3.75	0.00	0.00	0.00	0.00	0.00	0.21	3.78	3.55	1.59	0.59	0.03	0.03	0.00	0.00	0.00	0.00	9.78	7.38	5.68
4.0 - 4.5	4.25	0.00	0.00	0.00	0.00	0.00	0.00	0.95	2.54	1.41	0.46	0.06	0.01	0.00	0.00	0.00	0.00	5.42	7.79	4.27
4.5 - 5.0	4.75	0.00	0.00	0.00	0.00	0.00	0.00	0.16	1.39	1.02	0.39	0.14	0.00	0.00	0.00	0.00	0.00	3.09	8.16	3.18
5.0 - 5.5	5.25	0.00	0.00	0.00	0.00	0.00	0.00	0.00	0.57	0.96	0.29	0.22	0.05	0.00	0.00	0.00	0.00	2.09	8.64	2.78
5.5 - 6.0	5.75	0.00	0.00	0.00	0.00	0.00	0.00	0.00	0.09	0.70	0.27	0.11	0.07	0.00	0.00	0.00	0.00	1.23	8.99	2.05
6.0 - 6.5	6.25	0.00	0.00	0.00	0.00	0.00	0.00	0.00	0.01	0.68	0.62	0.10	0.14	0.00	0.00	0.00	0.00	1.56	9.29	3.16
6.5 - 7.0	6.75	0.00	0.00	0.00	0.00	0.00	0.00	0.00	0.00	0.22	0.50	0.08	0.09	0.00	0.00	0.00	0.00	0.88	9.54	2.15
7.0 - 7.5	7.25	0.00	0.00	0.00	0.00	0.00	0.00	0.00	0.00	0.04	0.50	0.10	0.03	0.00	0.00	0.00	0.00	0.66	9.67	1.88
7.5 - 8.0	7.75	0.00	0.00	0.00	0.00	0.00	0.00	0.00	0.00	0.02	0.34	0.09	0.04	0.00	0.00	0.00	0.00	0.48	9.81	1.58
8.0 - 8.5	8.25	0.00	0.00	0.00	0.00	0.00	0.00	0.00	0.00	0.00	0.27	0.02	0.02	0.00	0.00	0.00	0.00	0.30	9.67	1.11
8.5 - 9.0	8.75	0.00	0.00	0.00	0.00	0.00	0.00	0.00	0.00	0.00	0.07	0.05	0.00	0.00	0.00	0.00	0.00	0.11	9.90	0.48
9.0 - 9.5	9.25	0.00	0.00	0.00	0.00	0.00	0.00	0.00	0.00	0.00	0.04	0.06	0.00	0.00	0.00	0.00	0.00	0.10	10.09	0.47
9.5 - 10.0	9.75	0.00	0.00	0.00	0.00	0.00	0.00	0.00	0.00	0.00	0.00	0.01	0.00	0.00	0.00	0.00	0.00	0.01	10.50	0.06
All		0.00	0.00	0.00	3.51	9.98	24.73	25.22	17.65	11.07	5.97	1.31	0.52	0.00	0.00	0.00	0.00	99.97	6.60	42.3

8   Prediction model and coefficients

A numerical model has been developed to estimate the production. The applied model has been extensively validated in small scale basin tests [6, 11-13], and further by full scale tests in the North Sea with the Wavestar prototype in Hanstholm [7-10]. As described in [28] the prototype produced 45 MWh of electrical energy during the last year of operation, where the operational time was 88 %. The same model has been used for the cases but for an operational time of 88 % the model is giving 42 MWh/year.

As inputs to the model are a significant number of parameters, which contains realistic limits mainly on power production. Some of the input parameters are described in Section 4, but some of the, not so obvious, parameters are explained further in the following. The choices for the settings of these parameters are very important for the yearly energy production, as most of them are leading to a significant reduction in the power performance compared to a non-limited case. The actual values chosen for the cases has been selected in collaboration with specialists from Wavestar, based on the experiences with the Wavestar Hanstholm device. Hereby the output from the model in terms of yearly production are expected to be realistic.

- "Max control torque e6[Nm]". The value of this parameter is corresponding to the capabilities of the hydraulic cylinder. When forces are above this limit the pressure in the hydraulic system will pass over a relief valve, thereby ensuring that the cylinder and PTO system is not overloaded. The value is selected according to the capabilities by the hydraulic cylinder used by Wavestar.
- "Array interaction factor [-]". This is the q-factor for the array as described in Section 4.4 and Appendix A. Lay-outs with an increasing number of floats have reductions in the q-factor.
- "Storm protection [m]". The production is set to zero when waves are exceeding this limit, as the machine will be in storm protection.
- "Min. PTO power [kW]". The cut-in power. If the calculated power by the model is below the specified value it is set to zero, as the WEC would be placed in idle mode in reality without any production.
- "Max. PTO power [kW]" If the calculated production exceeds this level it will be set to the actual level according to the real capacity of the device.
- "Background consumption [kW]". Besides losses due to the PTO efficiency the device has a constant consumption all hours of the year. I.e. a yearly loss in energy corresponding to this value is calculated by multiplying with the number of hours in a year, i.e. 8760 hours. The losses for the background consumption is very significant to take into account, as it is corresponding to an additional loss of 2 to 5 % in the energy production on top of the direct losses caused by the PTO efficiency.
- "Part of time in production [%]". In some parts of the year the device will be out of operation due to maintenance, faults, errors, damages, etc. In the case studies it is assumed that operation is maintained in 95 % of the time. The time out of operation is assumed to be constantly distributed over the year (not depending e.g. on sea state), such that the calculated yearly production is simply reduced by 5 %.

9 Power matrices

The power matrices for the cases defined in Section 5 are given in Table 8 to 17. The model inputs described in Section 8 has been used.

*Table 8: Power matrix for **Reference case "Hanstholm"**.*

Machine: Electrical power [kW] — 100% operation, array interaction, power limit and storm protection limit

PTO efficiency [%]	Hm0 range [m]	Hm0 [m]	0-1	1-2	2-3	3-4	4-5	5-6	6-7	7-8	8-9	9-10	10-11	11-12	12-13	13-14	14-15	15-16
50	Wave period T0,2 [s]		0.5	1.5	2.5	3.5	4.5	5.5	6.5	7.5	8.5	9.5	10.5	11.5	12.5	13.5	14.5	15.5
Arm length [m] 10	0.0 - 0.5	0.25	0	0	0	0	0	0	0	0	0	0	0	0	0	0	0	0
Float diameter [m]	0.5 - 1.0	0.75	0	0	1	2	3	3	3	3	3	3	3	2	2	2	2	2
5	1.0 - 1.5	1.25	0	0	3	7	9	9	9	8	8	7	6	6	6	5	5	5
Scale	1.5 - 2.0	1.75	0	1	6	13	17	17	16	14	13	12	11	10	10	9	8	8
1.00	2.0 - 2.5	2.25	0	1	10	22	27	26	24	21	19	18	16	15	14	13	12	11
Storm protection [m]	2.5 - 3.0	2.75	0	2	15	33	38	36	32	29	26	24	22	20	18	17	16	15
3.00	3.0 - 3.5	3.25	0	0	0	0	0	0	0	0	0	0	0	0	0	0	0	0
	3.5 - 4.0	3.75	0	0	0	0	0	0	0	0	0	0	0	0	0	0	0	0
	4.0 - 4.5	4.25	0	0	0	0	0	0	0	0	0	0	0	0	0	0	0	0
	4.5 -	4.75	0	0	0	0	0	0	0	0	0	0	0	0	0	0	0	0

*Table 9: Power matrix for **Case A**.*

Machine: Electrical power [kW] — 100% operation, array interaction, power limit and storm protection limit

PTO efficiency [%]	Hm0 range [m]	Hm0 [m]	0-1	1-2	2-3	3-4	4-5	5-6	6-7	7-8	8-9	9-10	10-11	11-12	12-13	13-14	14-15	15-16
70	Wave period T0,2 [s]		0.5	1.5	2.5	3.5	4.5	5.5	6.5	7.5	8.5	9.5	10.5	11.5	12.5	13.5	14.5	15.5
Arm length [m] 12	0.0 - 0.5	0.25	0	0	0	0	0	11	11	11	11	10	0	0	0	0	0	0
Float diameter [m]	0.5 - 1.0	0.75	0	0	16	39	60	72	76	75	71	67	63	59	56	53	50	47
6	1.0 - 1.5	1.25	0	0	42	102	154	180	182	175	163	151	141	131	123	115	108	103
Scale	1.5 - 2.0	1.75	0	10	80	196	288	322	317	297	273	251	232	215	200	188	177	167
1.20	2.0 - 2.5	2.25	0	16	131	318	453	491	470	433	395	361	332	306	284	266	250	236
Storm protection [m]	2.5 - 3.0	2.75	0	24	194	467	644	678	637	580	525	477	437	402	373	349	327	308
3.50	3.0 - 3.5	3.25	0	34	270	644	859	880	814	735	662	599	547	503	466	434	407	383
	3.5 - 4.0	3.75	0	0	0	0	0	0	0	0	0	0	0	0	0	0	0	0
	4.0 - 4.5	4.25	0	0	0	0	0	0	0	0	0	0	0	0	0	0	0	0
	4.5 - 5.0	4.75	0	0	0	0	0	0	0	0	0	0	0	0	0	0	0	0

*Table 10: Power matrix for **Case B**.*

Machine: Electrical power [kW] — 100% operation, array interaction, power limit and storm protection limit

PTO efficiency [%]	Hm0 range [m]	Hm0 [m]	0-1	1-2	2-3	3-4	4-5	5-6	6-7	7-8	8-9	9-10	10-11	11-12	12-13	13-14	14-15	15-16
80	Wave period T0,2 [s]		0.5	1.5	2.5	3.5	4.5	5.5	6.5	7.5	8.5	9.5	10.5	11.5	12.5	13.5	14.5	15.5
Arm length [m] 12	0.0 - 0.5	0.25	0	0	0	11	16	20	20	21	21	20	20	19	18	17	16	16
Float diameter [m]	0.5 - 1.0	0.75	0	0	24	62	100	123	132	131	125	117	110	102	97	91	86	82
6	1.0 - 1.5	1.25	0	0	63	161	252	298	289	269	249	231	215	201	189	178	168	159
Scale	1.5 - 2.0	1.75	0	16	120	308	462	521	510	476	436	400	368	341	318	298	281	265
1.20	2.0 - 2.5	2.25	0	26	195	498	719	779	741	680	617	562	516	476	443	415	390	368
Storm protection [m]	2.5 - 3.0	2.75	0	38	288	730	1000	1000	991	898	810	734	671	619	574	536	503	474
3.50	3.0 - 3.5	3.25	0	53	402	991	1000	1000	1000	1000	1000	915	834	766	710	663	621	585
	3.5 - 4.0	3.75	0	0	0	0	0	0	0	0	0	0	0	0	0	0	0	0
	4.0 - 4.5	4.25	0	0	0	0	0	0	0	0	0	0	0	0	0	0	0	0
	4.5 - 5.0	4.75	0	0	0	0	0	0	0	0	0	0	0	0	0	0	0	0

*Table 11: Power matrix for **Case C**.*

Machine: Electrical power [kW] — 100% operation, array interaction, power limit and storm protection limit

PTO efficiency [%]	Hm0 range [m]	Hm0 [m]	0-1	1-2	2-3	3-4	4-5	5-6	6-7	7-8	8-9	9-10	10-11	11-12	12-13	13-14	14-15	15-16
90	Wave period T0,2 [s]		0.5	1.5	2.5	3.5	4.5	5.5	6.5	7.5	8.5	9.5	10.5	11.5	12.5	13.5	14.5	15.5
Arm length [m] 12	0.0 - 0.5	0.25	0	0	0	16	27	35	35	41	43	42	41	40	38	37	34	33
Float diameter [m]	0.5 - 1.0	0.75	0	0	33	92	158	203	219	215	205	192	179	169	158	150	141	134
6	1.0 - 1.5	1.25	0	12	87	240	390	466	472	448	416	383	354	329	308	290	273	259
Scale	1.5 - 2.0	1.75	0	23	166	456	699	788	767	711	649	593	545	505	471	443	417	394
1.20	2.0 - 2.5	2.25	0	37	270	730	1000	1000	1000	995	900	818	749	693	644	604	568	536
Storm protection [m]	2.5 - 3.0	2.75	0	55	399	1000	1000	1000	1000	1000	1000	1000	964	889	825	771	724	684
3.50	3.0 - 3.5	3.25	0	77	557	1000	1000	1000	1000	1000	1000	1000	1000	1000	1000	945	886	836
	3.5 - 4.0	3.75	0	0	0	0	0	0	0	0	0	0	0	0	0	0	0	0
	4.0 - 4.5	4.25	0	0	0	0	0	0	0	0	0	0	0	0	0	0	0	0
	4.5 - 5.0	4.75	0	0	0	0	0	0	0	0	0	0	0	0	0	0	0	0

*Table 12: Power matrix for **Case D**.*

Machine: Electrical power [kW] — 100% operation, array interaction, power limit and storm protection limit

PTO efficiency [%]	Hm0 range [m]	Hm0 [m]	0-1	1-2	2-3	3-4	4-5	5-6	6-7	7-8	8-9	9-10	10-11	11-12	12-13	13-14	14-15	15-16
90	Wave period T0,2 [s]		0.5	1.5	2.5	3.5	4.5	5.5	6.5	7.5	8.5	9.5	10.5	11.5	12.5	13.5	14.5	15.5
Arm length [m] 12	0.0 - 0.5	0.25	0	0	0	16	27	35	35	41	43	42	41	40	38	37	34	33
Float diameter [m]	0.5 - 1.0	0.75	0	0	33	92	158	203	219	215	205	192	179	169	158	150	141	134
6	1.0 - 1.5	1.25	0	12	87	240	390	466	472	448	416	383	354	329	308	290	273	259
Scale	1.5 - 2.0	1.75	0	23	166	456	699	788	767	711	649	593	545	505	471	443	417	394
1.20	2.0 - 2.5	2.25	0	37	270	730	1064	1150	1091	995	900	818	749	693	644	604	568	536
Storm protection [m]	2.5 - 3.0	2.75	0	55	399	1052	1473	1544	1436	1296	1166	1055	964	889	825	771	724	684
4.00	3.0 - 3.5	3.25	0	77	557	1435	1930	1963	1800	1612	1445	1302	1187	1091	1011	945	886	836
	3.5 - 4.0	3.75	0	103	744	1852	2000	2000	2000	1943	1735	1560	1418	1301	1204	1124	1053	993
	4.0 - 4.5	4.25	0	0	0	0	0	0	0	0	0	0	0	0	0	0	0	0
	4.5 - 5.0	4.75	0	0	0	0	0	0	0	0	0	0	0	0	0	0	0	0

*Table 13: Power matrix for **Case E**.*

Machine: Electrical power [kW] — 100% operation, array interaction, power limit and storm protection limit

PTO efficiency [%]	Hm0 range [m]	Hm0 [m]	0-1	1-2	2-3	3-4	4-5	5-6	6-7	7-8	8-9	9-10	10-11	11-12	12-13	13-14	14-15	15-16
90	Wave period T0,2 [s]		0.5	1.5	2.5	3.5	4.5	5.5	6.5	7.5	8.5	9.5	10.5	11.5	12.5	13.5	14.5	15.5
Arm length [m] 12	0.0 - 0.5	0.25	0	0	0	19	33	42	42	48	51	50	49	48	45	43	41	39
Float diameter [m]	0.5 - 1.0	0.75	0	0	39	109	188	242	260	256	244	228	213	200	188	178	168	160
6	1.0 - 1.5	1.25	0	14	103	285	464	553	560	532	493	454	420	391	366	344	325	307
Scale	1.5 - 2.0	1.75	0	27	197	541	830	936	911	845	771	704	648	600	560	526	495	468
1.20	2.0 - 2.5	2.25	0	44	321	867	1263	1366	1295	1181	1069	971	889	823	765	717	674	637
Storm protection [m]	2.5 - 3.0	2.75	0	65	474	1250	1749	1833	1706	1539	1385	1253	1145	1055	979	915	860	812
4.00	3.0 - 3.5	3.25	0	91	662	1704	2000	2000	2000	1915	1715	1546	1410	1296	1200	1122	1053	993
	3.5 - 4.0	3.75	0	122	883	2000	2000	2000	2000	2000	2000	1852	1683	1545	1430	1334	1251	1179
	4.0 - 4.5	4.25	0	0	0	0	0	0	0	0	0	0	0	0	0	0	0	0
	4.5 - 5.0	4.75	0	0	0	0	0	0	0	0	0	0	0	0	0	0	0	0

*Table 14: Power matrix for **Case F**.*

Machine: Electrical power [kW]							100% operation, array interaction, power limit and storm protection limit									
PTO efficiency [%]	Hm0 range [m]	Hm0 [m]	Wave period T0,2 [s]													
90			0-1	1-2	2-3	3-4	4-5	5-6	6-7	7-8	8-9	9-10	10-11	11-12	12-13	13-14	14-15	15-16
Arm length [m]			0.5	1.5	2.5	3.5	4.5	5.5	6.5	7.5	8.5	9.5	10.5	11.5	12.5	13.5	14.5	15.5
12	0.0 - 0.5	0.25	0	0	0	43	73	95	95	108	114	113	109	107	102	97	92	87
Float diameter [m]	0.5 - 1.0	0.75	0	0	88	244	422	543	583	574	547	512	478	449	422	399	377	358
6	1.0 - 1.5	1.25	0	32	232	639	1041	1243	1258	1195	1108	1021	944	878	822	773	729	690
Scale	1.5 - 2.0	1.75	0	61	442	1215	1863	2101	2045	1897	1732	1582	1454	1348	1257	1180	1111	1050
1.20	2.0 - 2.5	2.25	0	99	720	1948	2837	3068	2908	2653	2400	2180	1996	1847	1717	1610	1514	1430
Storm protection [m]	2.5 - 3.0	2.75	0	147	1065	2806	3928	4000	3830	3455	3109	2813	2571	2369	2199	2055	1931	1823
4.00	3.0 - 3.5	3.25	0	205	1486	3826	4000	4000	4000	4000	3852	3472	3165	2910	2696	2520	2364	2230
	3.5 - 4.0	3.75	0	273	1983	4000	4000	4000	4000	4000	4000	4000	3780	3470	3211	2997	2808	2648
	4.0 - 4.5	4.25	0	0	0	0	0	0	0	0	0	0	0	0	0	0	0	0
	4.5 - 5.0	4.75	0	0	0	0	0	0	0	0	0	0	0	0	0	0	0	0

*Table 15: Power matrix for **Case G**.*

Machine: Electrical power [kW]							100% operation, array interaction, power limit and storm protection limit									
PTO efficiency [%]	Hm0 range [m]	Hm0 [m]	Wave period T0,2 [s]													
90			0-1	1-2	2-3	3-4	4-5	5-6	6-7	7-8	8-9	9-10	10-11	11-12	12-13	13-14	14-15	15-16
Arm length [m]			0.5	1.5	2.5	3.5	4.5	5.5	6.5	7.5	8.5	9.5	10.5	11.5	12.5	13.5	14.5	15.5
12	0.0 - 0.5	0.25	0	0	0	51	87	112	112	129	135	134	130	127	121	116	109	104
Float diameter [m]	0.5 - 1.0	0.75	0	0	105	290	501	644	693	682	650	607	567	534	501	474	447	425
6	1.0 - 1.5	1.25	0	38	275	759	1236	1476	1494	1419	1316	1212	1121	1042	976	918	865	820
Scale	1.5 - 2.0	1.75	0	72	525	1443	2212	2495	2429	2252	2057	1878	1727	1600	1493	1402	1319	1247
1.20	2.0 - 2.5	2.25	0	118	855	2313	3369	3643	3454	3150	2851	2589	2371	2194	2039	1912	1798	1698
Storm protection [m]	2.5 - 3.0	2.75	0	174	1265	3332	4000	4000	4000	4000	3693	3341	3053	2814	2611	2441	2293	2165
4.00	3.0 - 3.5	3.25	0	243	1765	4000	4000	4000	4000	4000	4000	4000	3759	3455	3201	2992	2807	2648
	3.5 - 4.0	3.75	0	325	2355	4000	4000	4000	4000	4000	4000	4000	4000	4000	3813	3559	3335	3144
	4.0 - 4.5	4.25	0	0	0	0	0	0	0	0	0	0	0	0	0	0	0	0
	4.5 - 5.0	4.75	0	0	0	0	0	0	0	0	0	0	0	0	0	0	0	0

*Table 16: Power matrix for **Case H**.*

Machine: Electrical power [kW]							100% operation, array interaction, power limit and storm protection limit									
PTO efficiency [%]	Hm0 range [m]	Hm0 [m]	Wave period T0,2 [s]													
90			0-1	1-2	2-3	3-4	4-5	5-6	6-7	7-8	8-9	9-10	10-11	11-12	12-13	13-14	14-15	15-16
Arm length [m]			0.5	1.5	2.5	3.5	4.5	5.5	6.5	7.5	8.5	9.5	10.5	11.5	12.5	13.5	14.5	15.5
12	0.0 - 0.5	0.25	0	0	0	51	87	112	112	129	135	134	130	127	121	116	109	104
Float diameter [m]	0.5 - 1.0	0.75	0	0	105	290	501	644	693	682	650	607	567	534	501	474	447	425
6	1.0 - 1.5	1.25	0	38	275	759	1236	1476	1494	1419	1316	1212	1121	1042	976	918	865	820
Scale	1.5 - 2.0	1.75	0	72	525	1443	2212	2495	2429	2252	2057	1878	1727	1600	1493	1402	1319	1247
1.20	2.0 - 2.5	2.25	0	118	855	2313	3369	3643	3454	3150	2851	2589	2371	2194	2039	1912	1798	1698
Storm protection [m]	2.5 - 3.0	2.75	0	174	1265	3332	4000	4000	4000	4000	3693	3341	3053	2814	2611	2441	2293	2165
4.50	3.0 - 3.5	3.25	0	243	1765	4000	4000	4000	4000	4000	4000	4000	3759	3455	3201	2992	2807	2648
	3.5 - 4.0	3.75	0	325	2355	4000	4000	4000	4000	4000	4000	4000	4000	4000	3813	3559	3335	3144
	4.0 - 4.5	4.25	0	417	3025	4000	4000	4000	4000	4000	4000	4000	4000	4000	4000	4000	3875	3651
	4.5 - 5.0	4.75	0	0	0	0	0	0	0	0	0	0	0	0	0	0	0	0

*Table 17: Power matrix for **Case I,J,K**. Production for waves with $H_{m0} > 5.0$ m is zero due to storm protection limit.*

Machine: Electrical power [kW]							100% operation, array interaction, power limit and storm protection limit									
PTO efficiency [%]	Hm0 range [m]	Hm0 [m]	Wave period T0,2 [s]													
90			0-1	1-2	2-3	3-4	4-5	5-6	6-7	7-8	8-9	9-10	10-11	11-12	12-13	13-14	14-15	15-16
Arm length [m]			0.5	1.5	2.5	3.5	4.5	5.5	6.5	7.5	8.5	9.5	10.5	11.5	12.5	13.5	14.5	15.5
16	0.0 - 0.5	0.25	0	0	0	51	141	238	308	308	352	370	367	355	355	349	330	316
Float diameter [m]	0.5 - 1.0	0.75	0	0	124	336	658	982	1165	1242	1243	1210	1150	1090	1035	986	935	893
8	1.0 - 1.5	1.25	0	0	275	748	1459	2144	2490	2597	2549	2439	2293	2154	2029	1918	1814	1725
Scale	1.5 - 2.0	1.75	0	89	551	1495	2899	4012	4386	4388	4196	3930	3656	3411	3192	2998	2831	2684
1.60	2.0 - 2.5	2.25	0	145	895	2424	4665	6118	6461	6308	5935	5494	5082	4720	4404	4127	3886	3683
Storm protection [m]	2.5 - 3.0	2.75	0	212	1308	3535	6757	8462	8713	8358	7766	7131	6572	6082	5663	5306	4980	4720
5.00	3.0 - 3.5	3.25	0	299	1846	4916	9230	11103	11189	10575	9729	8890	8165	7542	7008	6548	6139	5802
	3.5 - 4.0	3.75	0	395	2438	6425	11895	13860	13742	12850	11743	10691	9793	9031	8377	7811	7316	6905
	4.0 - 4.5	4.25	0	507	3126	8160	14913	15000	15000	15000	13838	12561	11476	10564	9783	9108	8521	8043
	4.5 - 5.0	4.75	0	634	3912	10072	15000	15000	15000	15000	15000	14491	13217	12143	11228	10441	9760	9206

10 Energy production by future Wavestar WECs

Production estimations for the cases introduced in Section 5 are given in Table 18, where the production numbers are marked with the red box. In the following the production output marked by the red box is illustrated by explaining the numbers for *Case A:*

1) The first line is giving the production to grid: 1420 MWh/year. This is the output from the model using the specified inputs, the power matrix for *Case A* (Table 9), and the wave scatter diagram for the Belgian site (Table 3).

2) The second line is the full load factor (also often called the *capacity factor*[2]): 16 %. This value is calculated from the machine capacity (1000 kW), the total number of hours in a year (8760 hours) and the actual production (1420,000 kWh). The result is: 1420,000/(1000*8760) = 0.16, i.e. 16 %. This denotes that the yearly production corresponds to operation at full capacity in 16 % of the time.

3) The third line is the capture length: 30 m. This value is calculated from the actual production (1420,000 kWh), the average wave power (5.4 kW/m) and the number of hours in a year (8760 hours). The result is: 1420,000/(5.4*8760) = 30 m. This means that the produced energy corresponds to that all the wave power from a width of 30 m has been collected.

4) The fourth row is the efficiency: 25 %. This value is calculated from the number of floats (20), the diameter of the floats (6 m) and the capture length (30 m). The result is: 30/(20*6) = 0.25, i.e. 25 %. This indicates that the machine is able to collect 25 % of the power from the waves along a width corresponding to the number of floats multiplied by the float diameter.

Table 18: Energy production results for the cases. The output production numbers are marked with the red box.

		Hanstholm	Demonstrator 20 float Ø6			(Pre-)commercial 20 float Ø6		Commercial 60 float Ø6			Commercial 60 float Ø8		
	Case	Reference	A	B	C	D	E	F	G	H	I	J	K
	Perspective	-	3 years	4 years	5 years	6 years	6 years	6 years	7 years	7 years	8 years	10 years	10 years
Output	Production to grid [MWh/year]	42	1,420	2,240	3,120	4,440	5,250	11,600	13,300	16,400	30,900	34,500	54,500
	Full load factor [%]	4	16	26	36	25	30	33	38	47	23	26	42
	Capture length [m]	2	30	47	66	22	26	58	67	51	155	191	147
	Efficiency [%]	19	25	39	55	19	22	16	19	14	32	40	31
Machine	Number of floats [-]	2	20	20	20	20	20	60	60	60	60	60	60
	Scale	1.00	1.20	1.20	1.20	1.20	1.20	1.20	1.20	1.20	1.60	1.60	1.60
	Float diameter [m]	5	6	6	6	6	6	6	6	6	8	8	8
	Length of arm [m]	10	12	12	12	12	12	12	12	12	16	16	16
PTO settings	Max control torque e6[Nm]	1	2.1	2.1	2.1	2.1	2.1	2.1	2.1	2.1	6.6	6.6	6.6
	PTO efficiency [%]	50	70	80	90	90	90	90	90	90	90	90	90
	Power gain factor [-]	1	1	1.3	1.6	1.6	1.9	1.6	1.9	1.9	1.9	1.9	1.9
	Storm protection [m]	3	3.5	3.5	3.5	4	4	4	4	4.5	5	5	5
	Array interaction factor [-]	0.85	0.72	0.72	0.72	0.72	0.72	0.64	0.64	0.64	0.64	0.64	0.64
	Min. PTO power [kW]	0	10	10	10	10	10	30	30	30	50	50	50
	Max. PTO power [kW]	110	1,000	1,000	1,000	2,000	2,000	4,000	4,000	4,000	15,000	15,000	15,000
	Background consumption [kW]	0	10	10	10	20	20	50	50	50	100	100	100
	Part of time in production [%]	88	95	95	95	95	95	95	95	95	95	95	95
Site details	Site	DK-Roshage	Be-Mermaid	Be-Mermaid	Be-Mermaid	Fr-2611	Fr-2611	Fr-2611	Fr-2611	Fr-3268	Fr-2611	UK-EMEC	UK-100m
	Water depth [m]	5	33	33	33	29.1	29.1	29.1	29.1	20.4	29.1	50	100
	Wave Period T0,2 Avg [s]	3.9	4.3	4.3	4.3	7.5	7.5	7.5	7.5	7.0	7.5	5.9	6.6
	Wave Height Hm0 Avg [m]	0.88	1.22	1.22	1.22	1.73	1.73	1.73	1.73	2.24	1.73	1.83	2.76
	Wave Power Avg [kW/m]	2.6	5.4	5.4	5.4	22.7	22.7	22.7	22.7	36.6	22.7	20.6	42.3

The machines in the 11 cases have increasing production as seen on the plot in Figure 21, i.e. the production by the individual machines are expected to be increasing the more developed the machines are. The actual performance of the cases can be compared by looking at the normalised plots in Figure 22 and Figure 23.

---

[2] *The net **capacity factor** of a power plant is the ratio of its actual output over a period of time, to its potential output if it were possible for it to operate at full nameplate **capacity** continuously over the same period of time*, cf. [14].
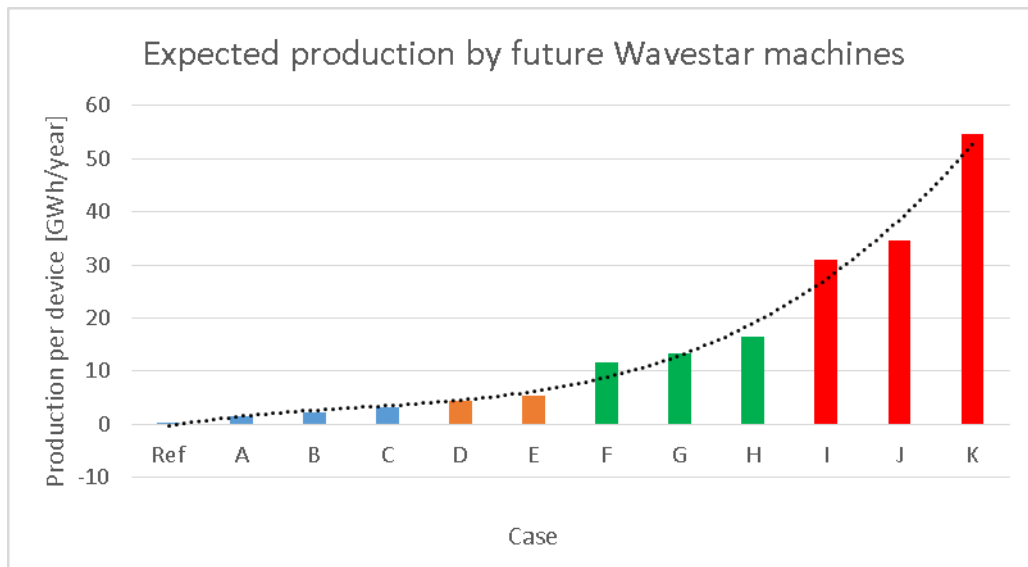
Figure 21: Production. The colouring of the bars indicate the level of development (ref Table 18).
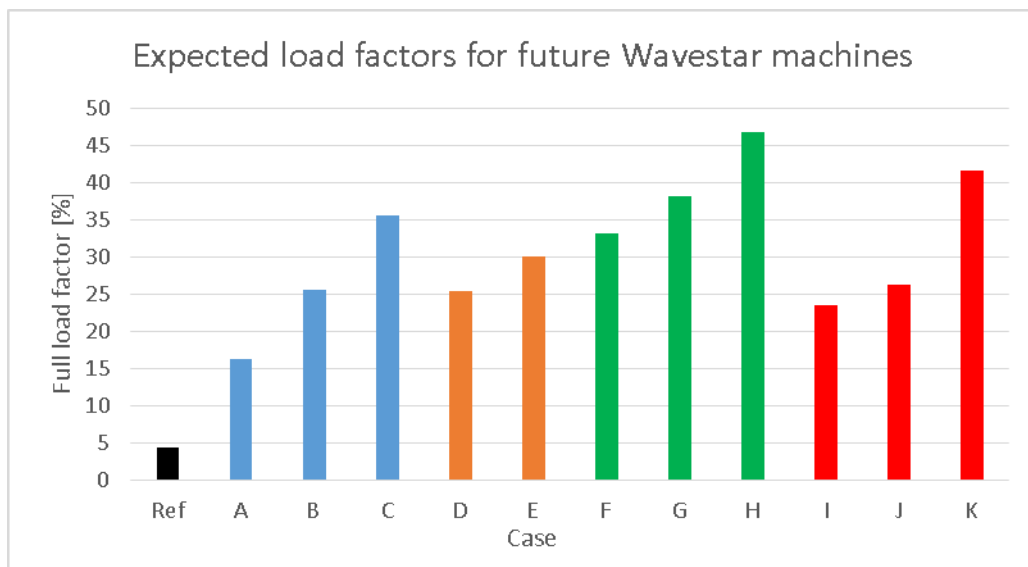

Figure 22: Load factors. The colouring of the bars indicate the level of development (ref Table 18).
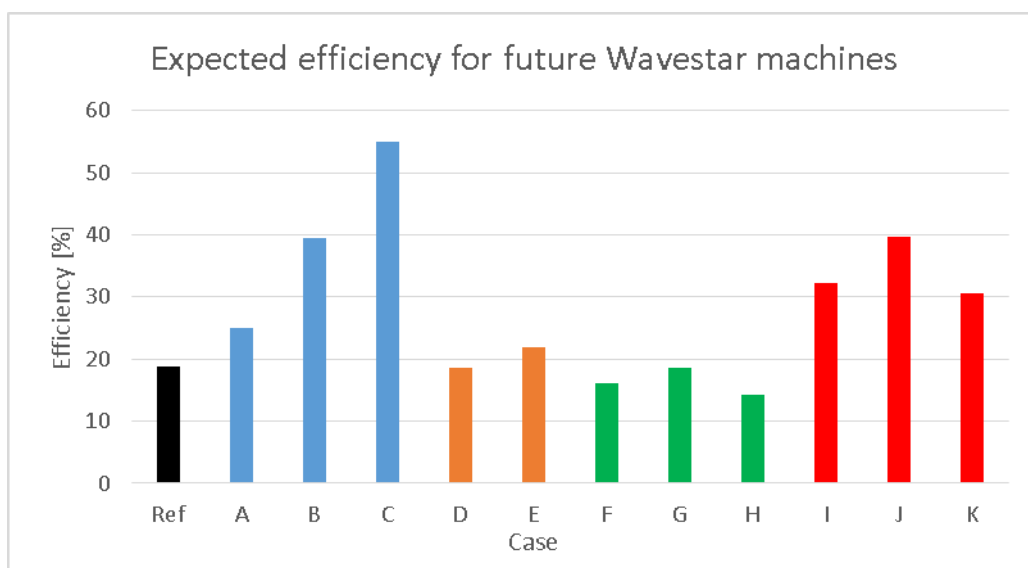

Figure 23: Efficiency. The colouring of the bars indicate the level of development (ref Table 18).

11 References

Some of the references below contain links to online web-pages. These links are only available in the electronic version (pdf) of this report.

[1]   Svendsen, R., Frigaard, P. (2001). *Indledende hydrauliske undersøgelser af bølgeenergianlægget Tusindben*. Aalborg Universitet, Laboratoriet for Hydraulik og Havnebygning.

[2]   Kramer, M. (2005).*Wave Star – Skala 1:40 modelforsøg, forsøgsrapport 3*. Hydraulics and Coastal Engineering No. 23. ISSN: 1603-9874. Aalborg University, Department of Civil Engineering, in Danish. Link, last visited January 22th 2016.

[3]   Frigaard, P. & Andersen, T.L. (2009). *Effektmålinger på Wave Star i Nissum Bredning*. Aalborg Universitet, Department of Civil Engineering, ISSN 1901-726X, DCE Technical Report No. 61.

[4]   Jakobsen, M.M., Kramer, M., Holk, N., Pedersen, M., Vidal, E. (2013). *MARINET Infrastructure Access Report, User-Project: AAUWS, Wave-Structure interactions on point absorber*. Marine Renewables Infrastructure Network, MARINET, Link , last visited January 14th 2016.

[5]   Jakobsen, M.M., Beatty, S., Kramer, M., Iglesias, G. (2016, in press). *MARINET Characterization of loads on a hemispherical point absorber wave energy converter*. International Journal of Marine Energy. IJOME-D-15-00017R1.

[6]   Jakobsen, M.M. (2015). *Wave-Structure Interactions on Point Absorbers – an experimental study*. Ph.D. Dissertation from Aalborg University, Department of Civil Engineering. Defended on 1st October 2015.

[7]   Kramer, M.M., Marquis, L., and Frigaard, P. (2011). *Performance Evaluation of the Wavestar Prototype*. EWTEC European Wave and Tidal Energy Conference, 2011.

[8]   Vidal, E., Hansen, R.H., Kramer, M.M. (2012). *Early Performance Assessment of the Electrical Output of Wavestar's prototype*. International Conference on Ocean Energy ICOE2012.

[9]   Wave Star A/S (2013). *Wavestar prototype at Roshage - Performance data for ForskVE project no 2009-1-10305 phase 1 & 2*. Project report for EnergiNet.dk ForskVE project no. 2009-1-10305. Link, last visited January 14th 2016.

[10] Marquis, L. (2014). *Wavestar- 4 years of continuous operation in the North Sea*. International Conference on Ocean Energy ICOE2014.

[11] Hansen, R.H. (2013). *Design and Control of the PowerTake-Off System for a Wave Energy Converter with Multiple Absorbers.* PhD-thesis from Department of Energy Technology, Aalborg University. Link, last visited January 14th 2016.

[12] Zurkinden, A. (2014). *Analysis of a Wave Energy Converter with Particular Focus on the Effects of Power Take-Off Forces on the Structural Responses*. Ph.D. Dissertation from Aalborg University, Department of Civil Engineering, ISSN 1901-7294, DCE Thesis no. 61. Link, last visited January 14th 2016.

[13] Ferri, F. (2014). *Wave-to-wire Modelling of Wave Energy Converters: Critical Assessment, Developments and Applicability for Economical Optimisation*. Dissertation from Aalborg University, Department of Civil Engineering, ISSN 1901-7294, DCE Thesis no. 60, Link, last visited January 14th 2016.

[14] Hansen, A.H., Clemmensen, H. (2015). *Energy Costs of Avoiding Pressure Oscillations in a Discrete Fluid Power Force System*. FPMC2015 Bath/ASME Symposium on Fluid Power & and Motion Control, October 12-14, 2015, Chicago, USA.

[15] Andersen, P., Pedersen, T.S., Nielsen, K.M., Vidal, E. (2015). *Model Predictive Control of a Wave Energy Converter*. MSC2015 conference, September, Sydney, Australia.

[16] Kramer, M. (2015). *Wave energy at Aalborg University*. Wave Energy International Business2Business Event WEIB2015, Aalborg University, Department of Civil Engineering, 28 April 2015.

[17] Hansen, A.H. (2014). Investigation and Optimisation of a Discrete Fluid Power PTO-system for Wave Energy Converters. ISBN 978-87-92846-44-0, PhD-thesis from Department of Energy Technology, Aalborg University. Link, last visited January 14th 2016.

[18] Vidal, E., Hansen, R.H., Kramer, M.M. (2015). *Control Performance Assessment and Design of Optimal Control to Harvest Ocean Energy*. Journal of Oceanic Engineering, IEEE, Volume 40.

[19] Nielsen, SRK., Zhou, Q., Basu, B., Sichani, MT., Kramer, MM. (2014). *Optimal Control of an Array of Non-Linear Wave Energy Point Converters*. Journal of Applied Ocean Research.

[20] Ferri, F., Ambühl, S., Kofoed, J.P. (2015). *Influence of the excitation force estimator methodology within a predictive controller framework on the overall cost of energy minimisation of a wave energy converter*. Proceeding at the International Conference on Computational Methods in Marine Engineering VI.

[21] Nambiar, A., Forehand, D., Kramer, M., Hansen, R., Ingram, D. (2014). *Effects of hydrodynamic interactions and control within a point absorber array on electrical output*. International Journal of Marine Energy 9.

[22] Nielsen, K., Jensen, M.S. (2004). *Wave Star Energy - WaveStar multi-float system performance calculation.* RAMBØLL technical report, Ref. No. FU4301, Link, last visited January 14th 2016.

[23] Ambühl, S. (2015). *Reliability of Wave Energy Converters*. PhD thesis, Department of Civil Engineering, Aalborg University. DCE Thesis, no. 70

[24] Holm, R.K., Berg, N.I., Walkusch, M., Rasmussen, P.O., Hansen, R.H. (2012). *Design of a magnetic lead screw for wave energy conversion*. XXth International Conference on Electrical Machines (ICEM), ISBN 978-1-4673-0143-5.

[25] Tetu, A. (2014). WaveSpring for enhancing wave energy absorption. Application to Danish Funding programme EUDP, project no. 64014-0156. Link, last visited January 20th 2016.

[26] Tona, P., Nguyen, H.N., Sabiron, G., Creff, Y. (2015). *An Efficiency-Aware Model Predictive Control Strategy for a Heaving Buoy Wave Energy Converter*. EWTEC European Wave and Tidal Energy Conference, 2015.

[27] Hansen, R., Kramer, M.M. (2011). *Modelling and Control of the Wavestar Prototype*. In Proc. EWTEC2011, The 9th European Wave and Tidal Energy Conference, Southampton, UK.

[28] Marquis, L., Kristensen, B., Sánchez, E.V. (2013). *Vision and Plans for Wavestar Development*. EWTEC European Wave and Tidal Energy Conference, 2013.

[29] Kramer, M., Brorsen, M., Frigaard, P. (2004). Wave Star - Indledende undersøgelse af flydergeometri. Hydraulics and Coastal Engineering No. 4, Aalborg University, Department of Civil Engineering, ISSN: 1603-9874, in Danish. Link, last visited January 22th 2016.

[30] Kramer, M., Andersen, T.L (2005). *Wave Star – Skala 1:40 modelforsøg, forsøgsrapport 2*. Hydraulics and Coastal Engineering No. 14. ISSN: 1603-9874. Aalborg University, Department of Civil Engineering, in Danish.

[31] Aqua-RET website. Aqua-RET 2 is an EU project funded through the Irish National Agency under the Lifelong Learning Programme. Link, last visited January 22th 2016.

[32] GENI website. Global Energy Network Institute. Link 1, Link 2, last visited January 22th 2016.

[33] UPWAVE project, Demonstration of a 1 MW wave energy converter integrated in an offshore wind turbine farm. EU financed project, Grant Agreement number: 691799 — UPWAVE — H2020-LCE-2014-2015/H2020-LCE-2015-2.

[34] Kracht, P. (2013). *Wave prediction and its implementation on control systems of Wave Energy Converters*. MARINET Infrastructure Access Report, Infrastructure: AAU Deep Water Wave Basin, User-Project: Adaptive WEC control, Marine Renewables Infrastructure Network, MARINET, Link , last visited January 27th 2016.

[35] Kracht, P. (2013). *Adaptive WEC control*. Fraunhofer IWES, Marine Renewables Infrastructure Network, MARINET, Link , last visited January 27th 2016.

[36] Kracht, P., Perez-Becker, S., Richard, J. & Fischer, B. (2015). *Performance Improvement of a Point Absorber Wave Energy Converter by Application of an Observer-Based Control: Results from Wave Tank Testing*. IEEE Transactions on Industry Applications, vol PP issue 99, Feb. 2015, 10. 1109/TIA.2015.2405892

[37] EMEC Orkney, The European Marine Energy Centre LTD, Link , last visited January 27th 2016.

[38] Matt Folley, Bjoern Elsaesser, Trevor Whittaker (2010). *Analysis of the wave energy resource at the European Marine Energy Centre*, 9th International Breakwater Conference, Edinburgh, UK. Link , last visited January 27th 2016.

[39] Cost of Energy (COE) Calculation Tool. Excel sheet and user guide. Link , last visited January 27th 2016.

[40] Nielsen K. and Pontes T. (2010). *Generic and Site-related Wave Energy Data*. Annex II. Task 1.1 International Energy Agency Ocean Energy Systems (IEA-OES).

[41] The Centre for Environment, Fisheries and Aquaculture Science (Cefas). [Online]. Link , last visited January 27th 2016.

[42] Wikipedia, capacity factor. Link , last visited January 27th 2016.

[43] WaveLab software from Aalborg University. Link, last visited January 27th 2016.

[44] 4C Offshore web-page. Link , last visited January 27th 2016.

[45] Beels, C. (2009). *Optimization of the Lay-out of a Farm of Wave Energy Converters in the North Sea - Analysis of Wave Power Resources, Wake Effects, Production and Cost*. PhD thesis from Department of Civil Engineering, Ghent University.

[46] Mathys, P., Rouck, J.D., Fernandez, L., Monballiu, J., Eynde, D.V.D., Delgado, R., Dujardin, A. (2012). *Belgian Ocean Energy Assessment BOREAS*. Project SD/NS/13, Belgian Science Policy Office, Link , last visited January 27th 2016.

[47] ANEMOC database. *Atlas Numérique d'Etats de mer Océanique et Côtier*, Link , last visited January 27th 2016.

[48] Andersen, M. T., & Frigaard, P.B. (2015). *Incentive-based Financial Support Scheme for Immature Renewable Energy Systems*. Proceedings of the 11th European Wave and Tidal Energy Conference.

Appendix A: Array interaction factors

This appendix summarizes some formulae and results for *Wavestar machine interaction factors*. The factor describes the power performance of a full machine with a given configuration (lay-out and number of floats) compared to a single float. The machine interaction factor depends on the control strategy, the wave spectrum, the wave direction and the machine configuration (lay-out and number of floats). As the device is not rotational symmetric, the wave direction is of importance, see Figure 24.
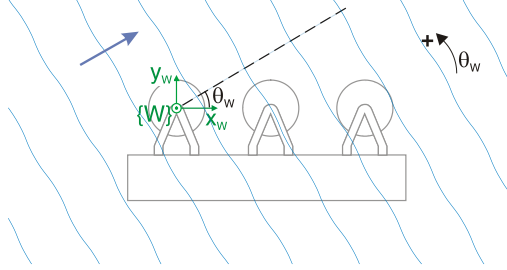
Figure 24: Definition of wave direction. Wave incidence 0° are for waves propagating along the x-axis (to the right).

The average power produced by a single float with $\theta_k = 0°$ is defined as the reference case. A "0" is included in the indexes to indicate this case. Index "*S*" is used for single float, and "*M*" is used for machine. The machine power is divided by the total number of floats *N1* to establish the *machine interaction factor*:

$$q_{M,k} = \frac{1}{N1} \frac{\overline{P_{M,k}}}{\overline{P_{S0,k}}}$$

- $q_{M,k}$: Machine array interaction factor [-]
- $\overline{P_M}$: Average power for machine in an irregular wave [W]
- $\overline{P_{S0}}$: Average power for a single float in an irregular wave with $\theta = 0°$ [W]
- $N1$: Total number of floats in machine
- Wave direction θ_k

In the following results are presented for the configurations shown in Table 19. The configurations are very different, and hereby the variation in machine power factors should reflect this diversity.

Table 19: Lay-outs used for investigation of q-factors.

Name	P-10	T-10	C-20	C-20Leg	E-21	E-27
Number of floats	10	10	20	20	21	27
Lay-out						

Factors based on linear assumptions will give reliable results for low wave heights, and for the yearly energy the factor is expected to be almost similar to factors that takes non-linearities into account (presumably an error of a few %). This appendix presents factors based on a linear approach:

- Calculations are done in the frequency domain
- Constraints are not included
  - PTO-moment is not limited
  - PTO efficiency is not taken into account
  - Power saturation limit is not included
- The PTO is assumed linear

As calculations are done in the frequency domain no simulations are necessary, and the results can be found by simple summations.

In Appendix A.1 formulae for power production in regular waves are presented, and in Appendix A.2 the formulae are extended to irregular waves. Appendix A.3 presents results of the array factor for the irregular waves.

Appendix A.1: Formulae for power in regular waves

For a linear system the power absorption is proportional to the motion amplitude squared. The absorbed average power for a single float in a regular wave is:

$$\overline{P_{SR,jk}} = \frac{1}{T}\int_0^T P_{inst}(t)\,dt \quad = \quad \frac{1}{2}\omega_j^2 c_c \left|A_{A,jk}\right|^2$$

- $\overline{P_{SR}}$: Average absorbed power for a single float in a regular wave [W]
- ω: Wave frequency [rad/s]
- c_c: Control damping gain [Nm/(rad/s)]
- A_A: Motion amplitude, complex [rad]
- j: Wave period T_j
- k: Wave direction θ_k

The power from all the floats in a machine is calculated by summing up the power from the total number of floats. For a machine with more than one float the motion amplitudes is represented by a column vector with $N1$ rows, and the control damping gain is a matrix. Hereby:

$$\overline{P_{MR,jk}} = \sum_{i=1}^{N1} \overline{P_{IR,ijk}} \quad = \quad \frac{1}{2}\omega_j^2 \cdot A_{A,jk}^T \cdot c_c \cdot A_{A,jk}^*$$

- $\overline{P_{MR}}$: Average absorbed power for machine in a regular wave [W]
- $\overline{P_{IR}}$: Average absorbed power for the individual floats in a regular wave [W]
- ω: Wave frequency [rad/s]
- c_c: Control damping gain, matrix [Nm/(rad/s)]
- A_A: Motion amplitude, complex vector with $N1$ rows [rad]
- $N1$: Total number of floats in machine
- i: Float number
- j: Wave period T_j
- k: Wave direction θ_k
- *"T"* in superscript*:* Transpose (not to be confused with the wave period)
- *"*"* in superscript*:* Complex conjugate

The motion amplitude depends on the float dynamics and the control gains, and it is calculated from the solution to the linear *equation of motion*. For a machine with multiple floats the hydrodynamic radiation, i.e. the added mass and damping, is represented by frequency dependant matrices of values. For a single float the matrices and vectors are just scalar values. The motion amplitude of the floats is found by:

$$A_{A,jk} = \left(K - \omega_j^2 M_j + i\omega_j C_j\right)^{-1} \cdot M_{e,jk}$$

- A_A: Motion amplitude, complex vector [rad]
- $M_e = H_{e,jk} \cdot A_{w,jk}$: Wave excitation moment, complex vector [Nm]
- ω: Wave frequency [rad/s]

- $K = k_h + k_c$: Stiffness, matrix [Nm/rad]
- $M = J + M_{h,j}$: Inertia, matrix [kgm²]
- $C = C_{h,j} + c_c$: Damping, matrix [Nm/(rad/s)]
- $H_{e\eta}$: Wave excitation force frequency response function, complex vector [Nm/m]
- A_w: Wave amplitude of incident wave [m]
- J: Mass inertia moment of float and arm, matrix [kgm²]
- M_h: Hydrodynamic added mass, matrix [kgm²]
- C_h: Hydrodynamic damping, matrix [Nm/(rad/s)]
- k_h: Hydrostatic stiffness, matrix [Nm/rad]
- k_c: Control stiffness, matrix [Nm/rad]
- c_c: Control damping, matrix [Nm/(rad/s)]
- j: Wave period T_j
- k: Wave direction θ_k

Appendix A.2: Formulae for power in irregular waves

The wave spectrum is discretized to provide wave amplitudes $A_{w,j}$ at the same frequencies as the wave excitation force frequency response function. This information is used to get rid of the dependency of the wave components (j). Because of the non-linearity in the power calculation, the wave amplitudes must be included inside the summations. For the single float the average power in the irregular wave is calculated by:

$$\overline{P_{S,k}} = \sum_{j=1}^{N2} \frac{1}{2} \omega_j^2 c_c \left| A_{A,jk} \right|^2$$

- $\overline{P_S}$: Average absorbed power for a single float in an irregular wave [W]
- j: Wave component given by the spectrum with period T_j and amplitude $A_{w,j}$
- $N2$: Total number of wave components in spectrum

In similar way for the complete machine:

$$\overline{P_{M,k}} = \sum_{i=1}^{N1} \overline{P_{I,\iota k}} = \sum_{j=1}^{N2} \frac{1}{2} \omega_j^2 \cdot A_{A,jk}^T \cdot c_c \cdot A_{A,jk}^*$$

- $\overline{P_M}$: Average absorbed power for machine in an irregular wave [W]
- $\overline{P_I}$: Average absorbed power for the individual floats in an irregular wave [W]
- i: Float number
- j: Wave component given by the spectrum with period T_j and amplitude $A_{w,j}$
- $N1$: Total number of floats in machine
- $N2$: Total number of wave components in spectrum

Appendix A.3: Results for selected lay-outs

Results are presented using irregular long crested waves based on the Pierson Moskowich spectrum with H_{m0} = 2.5 m and $T_{0,2}$ = 6.5 s at a water depth of 30 m. Coefficients for the equations (stiffness/inertia/mass matrices & wave excitation forces) have been calculated using a standard linear 3D potential boundary element method (WAMIT), and by using the structural characteristics of the Wavestar device with a float diameter of 6 m.

The choice of control gains have been determined using time domain simulations. PI control gains for a single float have been optimised for average electrical power under the influence of a constrained PTO-moment and a PTO efficiency of 70 %. These control gains have then subsequently been used in the frequency domain calculations for the arrays. The same gains have been applied for all the floats in the arrays no matter of lay-out and wave incidence. As demonstrated in [21] coordinated array control was found to increase the array q-factors significantly, so improvements of the present results by optimization of a coordinated array control are likely to be large. However, the present results are anyway useful to indicate the trend in the array factors when making arrays with increasing number of floats.

In Table 20 the q-factors are given depending on wave direction. It is seen that the factors vary a few % depending on direction. The last row in the table indicate the highest q-factor independent on direction. As the orientation of the lay-outs can be selected, it is chosen to base the trend in the q-factors on the best values.

The results are used in the main report Section 4.5, where the numbers are plotted in Figure 6 (on page 10).

Table 20: Array factors for the lay-outs. Reference for the factor is the single float at 0°.

Wave direction	Array factor q_M						
	Single float	P-10	T-10	C-20	C-20Leg	E-21	E-27
0°	1	0.85	0.94	0.65	0.65	0.70	0.66
45°	1.04	0.85	0.84	0.67	0.67	0.68	0.64
90°	1.07	0.85	0.77	0.71	0.72	0.69	0.65
135°	1.04	0.85	0.74	0.67	0.67	0.70	0.66
180°	1	0.85	0.79	0.65	0.65	0.68	0.63
225°	0.99	0.85	0.74	0.67	0.67	0.70	0.66
270°	0.99	0.85	0.77	0.71	0.72	0.69	0.65
315°	0.99	0.85	0.84	0.67	0.67	0.68	0.64
Best	1.07	0.85	0.94	0.71	0.72	0.70	0.66